DIGITAL ACCESS TO SCHOLARSHIP AT HARVARD

Candidates for Inelastic Dark Matter

(Article begins on next page)

Candidates for Inelastic Dark Matter

Yanou Cui, David E. Morrissey, David Poland, and Lisa Randall

Jefferson Physical Laboratory, Harvard University,
Cambridge, Massachusetts 02138, USA

August 17, 2009

Abstract

Although we have yet to determine whether the DAMA data represents a true discovery of new physics, among such interpretations inelastic dark matter (IDM) can match the energy spectrum of DAMA very well while not contradicting the results of other direct detection searches. In this paper we investigate the general properties that a viable IDM candidate must have and search for simple models that realize these properties in natural ways. We begin by determining the regions of IDM parameter space that are allowed by direct detection searches including DAMA, paying special attention to larger IDM masses. We observe that an inelastic dark matter candidate with electroweak interactions can naturally satisfy observational constraints while simultaneously yielding the correct thermal relic abundance. We comment on several other proposed dark matter explanations for the DAMA signal and demonstrate that one of the proposed alternatives – elastic scattering of dark matter off electrons – is strongly disfavored when the modulated and unmodulated DAMA spectral data are taken into account. We then outline the general essential features of IDM models in which inelastic scattering off nuclei is mediated by the exchange of a massive gauge boson, and construct natural models in the context of a warped extra dimension and supersymmetry.

Contents

1   Introduction

The DAMA/NaI and DAMA/LIBRA experiments observe an annual modulation signal in their NaI-based scintillation detectors with a statistical significance of $8.3\,\sigma$ [1]. A possible origin of this signal is galactic dark matter (DM) scattering off the nuclei in the detectors of these experiments [2, 3]. The annual variation would then result from the motion of the Earth relative to the Sun as it passes through the halo of dark matter enveloping our galaxy. The phase, period, and amplitude of the modulation signal seen by DAMA are all consistent with DM scattering [1]. We have yet to determine whether the observation is the result of truly new physics, or if it results from an unaccounted-for detector effect or background. In this paper, we ask the question: what if the DAMA result is truly a discovery of dark matter? What could it possibly be?

The major challenge for a DM interpretation of the DAMA result is that it appears to be at odds with the bounds on coherent DM-nucleus scattering obtained by other DM direct detection experiments such as CDMS [4] and XENON [5]. In contrast to DAMA, these experiments search for an unmodulated nuclear recoil signal from DM scattering using stronger background rejection methods. The bounds they place on DM-nucleon cross sections rule out coherent elastic scattering off iodine nuclei as the origin of the DAMA signal by several orders of magnitude. Lighter DM scattering coherently off sodium nuclei is marginally consistent with both DAMA and other experiments [6, 7], but gives a very poor fit to the energy spectrum of the modulated DAMA signal [8, 9, 10].

An elegant possibility that can account for the signal observed by the DAMA experiments that is also consistent with other direct detection experiments is dark matter that scatters *inelastically* off nuclei [11, 12, 13, 14]. In the inelastic dark matter (IDM) scenario, the dark matter particle χ_1 scatters preferentially off target nuclei into a slightly heavier χ_2 state. The kinematics of this process can enhance the nuclear recoil signal at DAMA relative to other experiments such as CDMS in a couple of ways. To produce a nuclear recoil signal with energy E_R, the minimum incident velocity of the DM particle is [11]

$$v_{min} = \frac{1}{\sqrt{2\,m_N\,E_R}} \left(\frac{m_N\,E_R}{\mu_N} + \delta \right),$$

(1.1)

where δ is the mass splitting between χ_1 and χ_2, m_N is the mass of the target nucleus, and μ_N is the reduced mass of the nucleus-DM system. The distribution of DM velocities in the galactic halo is expected to be approximately Maxwellian with an upper cutoff at the galactic escape velocity v_{esc} [3]. When the second term in this expression dominates, the minimal velocity needed to produce a recoil energy E_R is lower for heavier nuclei. This leads to an enhanced signal at DAMA, which contains iodine with $A \simeq 127$ as a detector material, relative to CDMS, consisting of germanium with $A \simeq 73$ [11]. The kinematics of inelastic DM scattering also increases the amount of annual modulation compared to the unmodulated signal rate, further enhancing the signal at DAMA relative to other direct detection experiments [11].

While IDM provides a compelling explanation for the DAMA signal, only a few concrete particle physics candidates have been proposed. A model with sneutrino DM where the

inelastic splitting is induced by the lepton-number violating superpotential operator $W \supset (L \cdot H_u)^2/\Lambda$ was suggested in Ref. [11]. Ref. [15] proposed that the inelasticity could arise from the radiative splitting of masses within a multiplet after the spontaneous breakdown of a new non-Abelian hidden gauge symmetry around a GeV. Pseudo-Dirac neutralinos as IDM arising from from approximately R-symmetric SUSY scenarios are considered in Refs. [16, 17].

In the present work we seek to obtain a broader overview of potential candidates for IDM. We study the general features required for IDM to account for the DAMA signal and we describe several explicit IDM candidates. To remain as general as possible, we do not attempt to account for the tantalizing indirect hints for dark matter such as the excess positron and electron fluxes observed by PAMELA [18], ATIC [19], and PPB-BETS [20], the INTEGRAL 511 keV line [21], or the WMAP haze [22, 23, 24]. In this paper our goal is simply to understand the possibilities for DAMA alone. What if DAMA represents a true discovery? What would be credible candidates for what it could be? It would of course be interesting to determine which of the candidates for IDM might be compatible with these indirect signals, but we postpone this direction to future work.

The outline of this paper is as follows. In Section 2 we investigate how well the hypothesis of IDM can account for the DAMA signal while evading the constraints from other direct detection searches for dark matter. We also argue that several other mechanisms proposed to explain this puzzle do not give a good fit to the full DAMA dataset. In Section 3 we discuss the general features required for a model to generate IDM, and we study the corresponding phenomenological constraints on these features. We present several plausible and explicit models that can give rise to IDM in Section 4. Section 5 is reserved for our conclusions.

2   Inelastic Dark Matter as an Explanation for DAMA

Inelastic dark matter has been shown to provide a compelling explanation for the signal in the DAMA experiments while remaining compatible with other direct DM searches such as CDMS, XENON, and CRESST for dark matter masses at least as large as 250 GeV [14]. Here we extend the analysis of Ref. [14] to larger dark matter masses. Such larger masses are of interest theoretically because they can be natural in the context of models addressing the hierarchy problem such as warped geometry [25] and supersymmetry [26]. In the case of electroweakly charged dark matter, they also lead to the correct thermal relic abundance. Additional attention to heavy dark matter is due to the recent experimental results from ATIC and PPB-BETS. We also consider some of the proposed alternative explanations of the DAMA signal and comment on their viability.

2.1   IDM Fits to the DAMA Data

We begin by reviewing the formalism for calculating the expected signal at direct detection experiments from the scattering of dark matter. The total rate of inelastic nuclear recoil

scatterings per unit mass of detector per unit recoil energy E_R in the lab frame is

$$\frac{dR}{dE_R} = N_T \frac{\rho_{DM}}{M_{DM}} \int_{v_{min}} d^3v \, v \, f(\vec{v}, \vec{v}_e) \frac{d\sigma}{dE_R}, \tag{2.1}$$

where $\rho_{DM} \simeq 0.3 \text{ GeV}/cm^3$ is the local DM density, M_{DM} is the DM mass, N_T is the number of target nuclei per unit mass of detector, and $f(\vec{v}, \vec{v}_e)$ is the local dark matter velocity distribution. For coherent spin-independent DM scattering, the DM-nucleus differential cross section $d\sigma/dE_R$ has the general form [27, 28]

$$\frac{d\sigma}{dE_R} = \frac{1}{v^2} \frac{m_N \, \sigma_n^0}{2\mu_n^2} \frac{\left[f_p \, Z + f_n \, (A - Z)\right]^2}{f_n^2} \, F^2(E_R), \tag{2.2}$$

where m_N is the mass of the target nucleus with atomic and molecular numbers A and Z, μ_n is the DM-nucleon reduced mass, f_p and f_n are effective coherent couplings to the proton and neutron, and σ_n^0 is the overall effective DM-neutron cross section at zero momentum transfer. The function $F^2(E_R)$ is a form factor characterizing the loss of coherence as the momentum transfer $q^2 = 2 \, m_N \, E_R$ deviates from zero. For computational simplicity, we use the Helm/Lewin-Smith [29, 30] parameterization of the form factor. In order to correct for the fact that this parameterization can be off by $\sim 20\%$ for larger values of E_R, we weight this by a quartic polynomial fit to the table given in [31], which gives the ratios of the Helm/Lewin-Smith form factor to the more accurate Two-Parameter Fermi (Woods-Saxon) form factor for various elements and values of E_R.

We take the DM velocity distribution to be Maxwellian with a cutoff [3],

$$f(\vec{v}, \vec{v}_e) = \frac{1}{(\pi \, v_0^2)^{3/2}} \, e^{-(\vec{v} + \vec{v}_e)^2/v_0^2} \, \Theta(v_{esc} - |\vec{v} + \vec{v}_e|). \tag{2.3}$$

Here, $v_0 \simeq 220 \, km/s$ is the DM *rms* speed, v_{esc} is the local DM *escape velocity* in the halo frame, $\vec{v}_e$ is the velocity of the Earth with respect to the galactic DM halo, and $\vec{v}$ is the DM velocity in the Earth frame. The signals from IDM are extremely sensitive to the value of v_{esc}, which is thought to be in the range $498 \, km/s < v_{esc} < 608 \, km/s$ [32]. The velocity of the Earth relative to the halo, $\vec{v}_e$, has components from both the motion of the solar system relative to the halo as well as the annual motion of the Earth about the Sun,

$$\vec{v}_e(t) = \vec{v}_s + V_o \left[\hat{\epsilon}_1 \cos(2\pi(t - t_1)) + \hat{\epsilon}_2 \sin(2\pi(t - t_1))\right] \tag{2.4}$$

where $\vec{v}_s \simeq (0, 220, 0) + (10, 5, 7) \, km/s$ is the velocity of the solar system relative to the halo [33, 34], $V_o \simeq 29.79 \, km/s$ is the Earth's orbital speed [30], and t is measured in years. Following the conventions of Ref. [35] and the discussion in Ref. [10], we are using coordinates where $\hat{x}$ points to the center of the galaxy, $\hat{y}$ gives the direction of disk rotation, and $\hat{z}$ points to the north galactic pole. The directions of the Earth's motion on $t_1 =$ March 21 ($\hat{\epsilon}_1$) and June 21 ($\hat{\epsilon}_2$) are given by $\hat{\epsilon}_1 = (0.9931, 0.1170, -0.01032)$ and $\hat{\epsilon}_2 = (-0.0670, 0.4927, -0.8678)$ [35].

The annual variation of the scattering rate due to $\vec{v}_e(t)$ is very nearly sinusoidal and we estimate the amplitude of the modulated rate to be

$$S \equiv \left.\frac{dR}{dE_R}\right|_{mod} \simeq \frac{1}{2} \left[\frac{dR}{dE_R}(June\ 2) - \frac{dR}{dE_R}(Dec\ 2)\right]. \tag{2.5}$$

When computing the unmodulated rate for a given experiment, we integrate the total rate over the time periods that the experiment recorded data. To convert rates to detector signals, we rescale by the efficiency of the detector and account for *quenching*, but we do not include any detector resolution effects. In addition, we have included a correction for channeling effects at DAMA, but find them to be unimportant for the range of parameters we consider.[1]

To determine the extent to which IDM can account for the DAMA signal, we compute the modulated recoil spectrum of IDM candidates and compare this to the energy spectrum in the twelve lowest bins in the $2-8$ keVee range reported by DAMA in Ref. [1]. For a given dark matter particle mass, we use a χ^2 *goodness-of-fit* metric to determine the 90% and 99% confidence level allowed regions. We define this metric as

$$\chi^2 \equiv \sum_{i=1}^{12} \frac{(S^i - S^i_{data})^2}{(\sigma^i_{data})^2}, \qquad (2.6)$$

where S^i denotes the average of the left, center, and right values of S in the ith 0.5 keV width bin, and σ^i_{data} the reported uncertainty in the measurement. For each value of the dark matter mass, we scan over 2 parameters (the overall nucleon cross section σ^0_n, and the mass splitting δ), so we require that $\chi^2 < 16.0\,(23.2)$ at the $90\,(99)\%$ level for $12 - 2 = 10$ degrees of freedom. We only consider signals from the scattering off of iodine, as it is expected to completely dominate for the parameters of interest to us. Following Ref. [14], we take the quenching factor for iodine to be $q_I = 0.085$.

As well as fitting to the DAMA results, we also compute the signals that each IDM candidate would produce at the CDMS experiments [37, 38, 4], CRESST-II [39], and ZEPLIN-III [40]. This imposes further constraints on the properties of a potential IDM candidate.[2] In order to be conservative in excluding IDM parameter space, we will assume that the small number of events seen by these experiments are signal events, and use Poisson statistics to find the region of parameter space excluded at the 99% confidence level based on the number of observed events.

CDMS has published data from three runs at the Soudan Underground Laboratory with approximate exposures of 19.4 kg-day [37], 34 kg-day [38], and 121.3 kg-day [4]. In total, these experiments reported two events between $10\,\mathrm{keV}$ and $100\,\mathrm{keV}$, which we assume to be signal. We thus require that the expected total number of events, integrated over the time the experiments ran, obeys $N_{tot} < 8.4$ at the 99% confidence level. We only consider scattering off germanium as it is expected to dominate for the heavier dark matter we consider.

CRESST-II has published data from a run in 2004 using prototype detector modules [43] and more recently has published results from a commissioning run carried out in 2007 [39]. Since there were significant changes to the detector modules between these runs, including

---

[1]The fraction of channeled events falls quickly with recoil energy, and can be approximated for iodine as $f_I \simeq 10^{-\sqrt{E_R/(11.5\,\mathrm{keV})}}$ [36, 10]. Since IDM suppresses scattering processes with low E_R, one expects only a very small number of channeled events.

[2]As in the analysis of Ref. [14], we find that the constraints from other experiments such as XENON10 [5], KIMS [41], and ZEPLIN-II [42] are currently not as important so we have not included them in our plots.

the addition of neutron shielding, we opt not to combine these data sets and consider constraints only from the later commissioning run, which had an exposure of 47.9 kg-day and an acceptance of 0.9 for tungsten recoils.[3] Taking the seven observed events between 12 keV and 100 keV to be signal, we require that the total number of predicted tungsten recoil events, integrated over the duration of the experiment, obeys $N_{tot} < 16.0$ at the 99% confidence level.

The ZEPLIN-III experiment has recently released data from a run in 2008 with an effective exposure of 126.7 kg-day [40]. The experiment observed seven events in its liquid xenon detector between 2 keVee and 16 keVee, so we require that the total number of events obeys $N_{tot} < 16.0$ at the 99% confidence level. To convert measured energy E_d to recoil energy E_R, we use the energy-dependent quenching factor given in Fig. 15 of Ref. [40], which saturates at $q_{Xe} \simeq 0.48$ around $E_d = 10$ keVee. Below this scale, we use the parametrization $q_{Xe} \approx (0.142\, E_d + 0.005)\, \mathrm{Exp}[-0.305\, E_d^{0.564}]$ given in Eq. (4.3) of Ref. [44], which we find gives a good fit to the curve.

In Figs. 1 and 2 we show the region allowed by DAMA and constraints from CDMS II, CRESST-II, and ZEPLIN-III at the fiducial point $f_n = f_p$ for various values of the dark matter mass between 100 GeV and 5 TeV. (Note that ultimately the relation between f_n and f_p is model-dependent, but we make this choice to allow a straightforward comparison to previous work [6, 7, 11, 12, 13, 14].) In addition, we consider escape velocities of 500 km/s and 600 km/s. We observe that while the relative constraints from CDMS II, CRESST-II, and ZEPLIN-III become stronger for heavier dark matter candidates, very heavy dark matter is not ruled out. While both the required cross section for DAMA and the constraint curves move upwards for heavier dark matter, they do so at roughly the same rate. One can understand this asymptotic behavior as follows. For large values of the dark matter mass relative to the mass of the nucleus, the reduced mass in Eq. (1.1) becomes $\mu_N \simeq m_N$ and is independent of the dark matter mass. Therefore the only mass dependence is in the prefactor of Eq. (2.1) which is the same for all experiments, so the constraint curves from different experiments do not move relative to each other.

It is quite interesting that heavier dark matter may be allowed – this opens up the possibility of simple dark matter models for which heavier masses are preferred for getting the right thermal relic abundance, or for explaining indirect signals such as the $e^+ + e^-$ excess at $\sim 300 - 800$ GeV seen by ATIC and PPB-BETS. Models addressing the hierarchy problem also often prefer heavier dark matter candidates [25, 26].

We stress, however, that the results of the present section depend on a number of astrophysical and nuclear physics quantities that are not fully understood and have large uncertainties. The size of the modulated signal at DAMA is particularly sensitive to the local dark matter velocity distribution. For example, as one can see from Figs. 1 and 2, increasing the halo escape velocity from 500 km/s to 600 km/s significantly tightens the constraints from CDMS. This is because inelastic DM scattering requires one to sample from the tail of the velocity distribution, especially for lighter target elements. Deviations from the assumed

---

[3]We note that the combined data sets would allow parameter points that are ruled out according to the later commissioning run considered in isolation due to the large number of observed events in the earlier run (5) relative to its exposure (20.5 kg-day).

Figure 1: Allowed regions for fits of inelastic dark matter to the DAMA data, as well as constraints from CDMS II, CRESST-II, and ZEPLIN-III. We fix the local DM density at $\rho = 0.3 \, \mathrm{GeV}/cm^3$, and vary the DM mass and escape velocity. These plots assume the relation $f_p = f_n$.
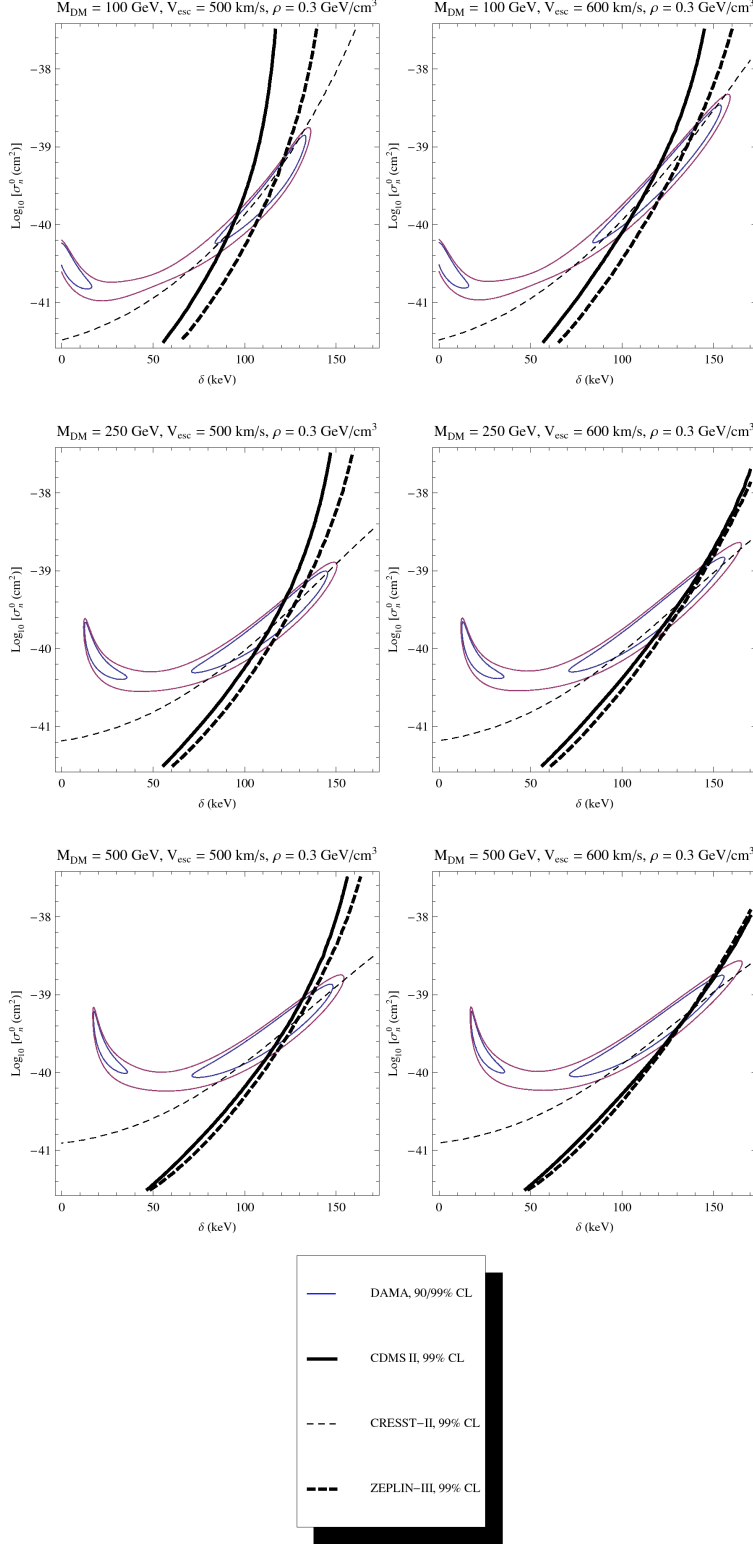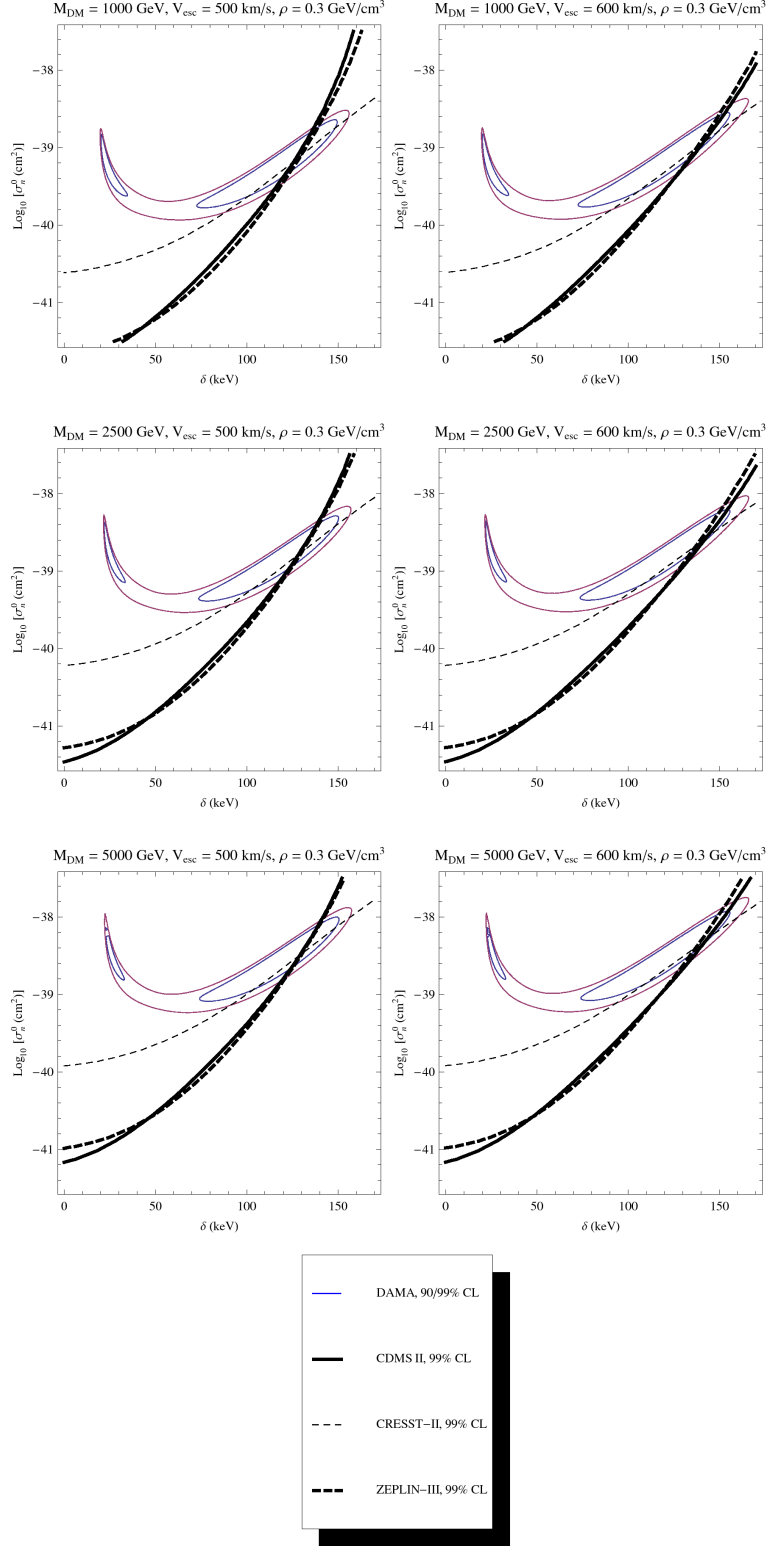
Figure 2: Allowed regions for fits of inelastic dark matter to the DAMA data, as well as constraints from CDMS II, CRESST-II, and ZEPLIN-III. We fix the local DM density at $\rho = 0.3\,\mathrm{GeV}/cm^3$, and vary the DM mass and escape velocity. These plots assume the relation $f_p = f_n$.

9

Maxwellian distribution at high velocities, as well as additional DM substructures such as streams or sub-halos, can also significantly affect the allowed region [45, 46, 47, 44]. For this reason, we have been extremely conservative in identifying the excluded region by using a *goodness-of-fit* estimator and only showing 99% confidence level exclusion contours for CDMS II, CRESST-II, and ZEPLIN-III. Given the uncertainties, it would be premature to rule out a broader range of IDM parameter space.

A second important uncertainty is the value of the local dark matter density ρ_{DM}, which is known only up to a factor of ~ 2. Varying ρ_{DM} will affect the overall normalization of the cross section σ_n^0 in the plots of Figs. 1 and 2 by a factor inversely proportional to it. While this is not terribly important for demonstrating the existence of an allowed region, since it affects all signals equally, the uncertainty in ρ_{DM} can be very important when comparing the allowed region to a model that predicts a specific value for σ_n^0.

Finally, we wish to emphasize that the analysis performed in this section (and in Refs. [14, 10, 44]) is not model-independent. Simple models of IDM, for example dark matter charged under $SU(2)_L$, will not respect the relation $f_p = f_n$, and the curves in Figs. 1 and 2 will move around by different amounts that depend on the atomic numbers relevant to the experiment. In Section 3, we will redo the analysis for dark matter charged under $SU(2)_L$, which scatters through Z^0-exchange. There we will see that when one considers the heavier dark matter masses that yield the correct thermal relic abundance [48], the scattering cross section from Z^0-exchange is tantalizingly close to the DAMA preferred region (which remains qualitatively similar to the $f_p = f_n$ case considered here).

2.2   Other DM Explanations for DAMA

In addition to IDM, a number of other non-standard DM candidates have been suggested as possible sources for the DAMA signal. These include lighter spin-independent elastic DM [6], lighter spin-dependent elastic DM [49], and elastic scattering off atomic electrons [50]. These alternatives to IDM turn out to be extremely strongly constrained when spectral data from DAMA is included in the analysis [8, 9, 10].

Light $2-10$ GeV elastic, spin-independent DM was proposed as an explanation for the DAMA signal in Ref. [6]. The DAMA signal in this scenario comes primarily from the light DM scattering off sodium rather than iodine. Such a light DM state would produce recoils near the lower end of the sensitivity range of most other direct detection experiments which consist of heavier target nuclei, strongly suppressing their signals relative to DAMA. The effect of light DM on DAMA can be further enhanced relative to other direct detection probes by *channeling*, which effectively reduces the amount of quenching in the DAMA target, leading to more events in the range of sensitivity [7].

However, subsequent analyses taking into account the modulated and unmodulated single-hit DAMA energy spectra indicate that this light DM scenario is strongly disfavored. It is found that light DM either does not provide a good fit to the modulated spectrum or predicts an unmodulated single-hit rate in the lowest energy bins that is much larger than the total rate observed by DAMA [8]. Even so, light spin-dependent DM may still be viable

if channeling is included [10].

A second alternative explanation for the DAMA result consists of moderately heavy $(m_{DM} \gtrsim 10 \text{ GeV})$ elastic DM that scatters primarily off atomic electrons rather than nuclei [50]. The vast majority of these scatterings would produce an electromagnetic signal in the DAMA detector in the eV energy range, well below the keV energies to which this detector is sensitive. However, the scattering of a halo DM particle off an atomic electron with an unusually high momentum in the tail of its distribution, on the order of an MeV, can generate a detected electromagnetic signal at DAMA of $E_d \sim$ few keV [50]. No such signal would have been recorded in other direct detection experiments such as CDMS and XENON since these experiments are careful to filter out electromagnetic events that they expect to arise from backgrounds. Electron scattering DM is also attractive in light of the PAMELA results [51, 52], which can be interpreted as coming from DM annihilating preferentially into leptons [53, 54].

Following the analysis of Ref. [8] for light DM scattering off nuclei, we investigate whether electron interacting DM is consistent with the modulated and unmodulated single-hit DAMA energy spectra. In our analysis we compute the modulated and unmodulated rates for DM scattering off electrons as in Ref. [50]. We compare our binned results to the lowest twelve 2–8 keVee DAMA modulated bins and the lowest six 0.875–2.125 keVee DAMA unmodulated single-hit bins using a modified χ^2 measure. We use a standard χ^2 *goodness-of-fit* measure for the modulated bins, while for the unmodulated bins we add to the χ^2 only if the predicted signal is larger than the observed value to allow for an unmodulated background. This procedure is very conservative in that it will only underestimate the excluded regions.

We find that under the assumptions about the DM made in Ref. [50], namely that the DM is fermionic and interacts with quarks by the exchange of a scalar or a gauge boson with $(V \pm A)$ couplings,[4] electron-interacting DM as an explanation for DAMA is excluded well beyond the 99% confidence level. This occurs for precisely the same reasons that light elastic DM is strongly disfavored: either the modulated signal is too low, or the unmodulated single-hit signal (*i.e.*, the signal excluding multiple scintillation events) exceeds the total rate observed by DAMA. In the present case, the signal rate falls quickly with increasing detected energy E_d because the momentum distribution of atomic electrons decreases rapidly in the relevant range, approximately as p^{-8} [50].

This tension is illustrated in Fig. 3 where we show the best fit (lowest effective χ^2) to the full DAMA spectral dataset (Fit A), as well as the best fit (lowest effective χ^2) to the modulated dataset alone leaving out the lowest 2 keVee energy bin (Fit B). In making these fits, we assume either chiral vector $(V \pm A)$ or scalar four-fermion interactions between the electron and a fermionic DM particle of mass equal to 200 GeV. However, the shape of the predicted spectrum, which is the source of the tension with the DAMA data, is effectively independent of the DM mass provided it is heavier than about 10 GeV [50]. Therefore the curves in Fig. 3 also apply to other DM masses provided we rescale the effective DM-electron coupling strength appropriately.

Our conclusion that electron-DM scattering gives a poor fit to the DAMA spectral data

---

[4]We also neglect parts of the electron-DM cross section suppressed by the DM velocity.
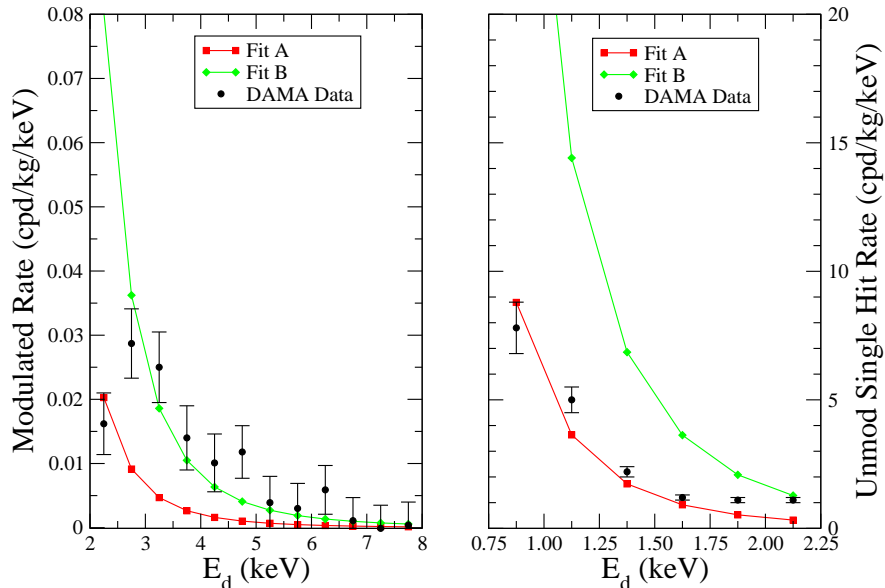
Figure 3: DAMA modulated and unmodulated single hit spectral data and fits of electromagnetic elastic DM scattering. The DM particle is assumed to be a fermion of mass $M_{DM} = 200$ GeV with either scalar or chiral vector $(V \pm A)$ couplings to electrons. The (red) curve for Fit A is the one that yields the lowest effective χ^2 value using both the modulated and single-hit unmodulated spectral data sets. The (green) curve for Fit B corresponds to that with the lowest effective χ^2 for the modulated dataset alone, excluding the lowest energy bin.

is robust. We find that it continues to hold even if we do not include the lowest modulated energy bin and the two lowest unmodulated energy bins in the fit. Furthermore, we have also examined other Dirac structures for the couplings between a fermionic DM particle and the target electron (relative to the scalar and vector $(V \pm A)$ couplings considered above and in Ref. [50]), and we find that these do not improve the situation. A scalar DM particle scattering elastically off electrons does not appear to work either.[5]

3   General IDM Properties and Nucleon Scattering

Having found that IDM provides an acceptable fit to the DAMA modulated and unmodulated spectral datasets and that other proposals are strongly constrained, we turn now to the general properties of potential IDM candidates. Clearly, any such candidate must have an inelastic nucleon-scattering cross section that is significantly enhanced relative to its elastic

---

[5] Inelastic dark matter scattering off electrons might work, although this would likely require an extremely large electron scattering cross section.

cross section. To meet these criteria, the mass, inelastic splitting, and inelastic cross section must all fall into the appropriate ranges. We now show these requirements can be satisfied by IDM particles in the mass range $100\,\mathrm{GeV} - 5\,\mathrm{TeV}$ that interact coherently with nuclei primarily through the exchange of a massive gauge boson.

3.1 Inelastic Interactions from a Massive Gauge Boson

When the DM-nucleon scattering is mediated by a massive gauge boson, the dominance of inelastic interactions over elastic arises in a natural way. We consider two types of IDM in this context: a Dirac fermion that is split into a pair of nearly degenerate Majorana states by a small Majorana mass, and a complex scalar that is split into two real scalars by a small holomorphic mass.[6]

For the fermion case, the models we consider all reduce to

$$\mathscr{L} \supset \bar{\psi} i \gamma^{\mu}(\partial_{\mu} + ig Q\, Z'_{\mu})\psi - M\bar{\psi}\psi - \frac{1}{2}m_L\left(\bar{\psi}^c P_L \psi + h.c.\right) - \frac{1}{2}m_R\left(\bar{\psi}^c P_R \psi + h.c.\right), \quad (3.1)$$

where ψ is a Dirac fermion, $M \gg m_{L,R}$, and Z'_{μ} is a massive gauge boson. The Majorana masses $m_{L,R}$ in Eq. (3.1) split the Dirac state ψ into a pair of Majorana states $\Psi_{1,2}$. In terms of these mass eigenstates, the Lagrangian becomes

$$\begin{aligned}
\mathscr{L} \;\supset\; & \frac{1}{2}\bar{\Psi}_1 i\gamma^{\mu}\partial_{\mu}\Psi_1 - \frac{1}{2}(M - m_+)\bar{\Psi}_1\Psi_1 \\
& + \frac{1}{2}\bar{\Psi}_2 i\gamma^{\mu}\partial_{\mu}\Psi_2 - \frac{1}{2}(M + m_+)\bar{\Psi}_2\Psi_2 \\
& + i\,g\,Q\,Z'_{\mu}\,\bar{\Psi}_2\gamma_{\mu}\Psi_1 \\
& + \frac{1}{2}\,g\,Q\,Z'_{\mu}\,\frac{m_-}{M}\left(\bar{\Psi}_2\gamma^{\mu}\gamma^5\Psi_2 - \bar{\Psi}_1\gamma^{\mu}\gamma^5\Psi_1\right) + \mathcal{O}\left(\frac{m^2}{M^2}\right),
\end{aligned} \qquad (3.2)$$

where $m_{\pm} = (m_L \pm m_R)/2$.

From this we see that the dominant gauge boson interaction is strictly off-diagonal, and that the mass splitting between the eigenstates is

$$\delta = M_2 - M_1 = 2\,m_+ = m_L + m_R. \qquad (3.3)$$

There is also a residual diagonal coupling of the fermions to the gauge boson, but it is suppressed by a power of $m_-/M \ll 1$.

The basic story for the scalar case is very similar. Consider the interactions

$$\mathscr{L} \supset |(\partial_{\mu} + igQ\,Z'_{\mu})\phi|^2 - M^2|\phi|^2 - \frac{1}{2}m^2(\phi^2 + h.c.), \qquad (3.4)$$

---

[6]Another interesting possibility would be spin 1 inelastic dark matter, but models of this type are more complicated.

where, again, Z'_μ is a massive vector boson and we assume $M^2 \gg m^2$ with m^2 real and positive. The holomorphic m^2 mass term splits the real and imaginary components of the complex scalar $\phi = (\phi_R + i\phi_I)/\sqrt{2}$. In terms of these fields, the Lagrangian becomes

$$\mathscr{L} \supset \frac{1}{2}(\partial\phi_R)^2 - \frac{1}{2}(M^2 + m^2)\phi_R^2 + \frac{1}{2}(\partial\phi_I)^2 - \frac{1}{2}(M^2 - m^2)\phi_I^2 \tag{3.5}$$

$$-gQ Z'^{\mu}(\phi_I \partial_\mu \phi_R - \phi_R \partial_\mu \phi_I) + \frac{1}{2}g^2 Q^2 Z'_\mu Z'^\mu (\phi_R^2 + \phi_I^2).$$

From this, we see that the single gauge boson interaction with two scalars is strictly off-diagonal, coupling ϕ_R exclusively to ϕ_I. The splitting between these mass eigenstates is

$$\delta = \sqrt{M^2 + m^2} - \sqrt{M^2 - m^2} \simeq \frac{m^2}{M}. \tag{3.6}$$

Let us also emphasize that in both the fermion and scalar IDM cases, it is technically natural to have the "Dirac" mass M much larger than the "Majorana" mass m. In the limit $m \to 0$, both theories have a global $U(1)_{DM}$ symmetry analogous to baryon number in the SM, implying that all quantum corrections to m (or m^2) are proportional to itself. Indeed, within the MSSM the B and L global symmetries keep the real and imaginary components of the squarks and sleptons degenerate, while the VEVs of the Higgs complex scalars split their components. In Section 4, we will construct models that generate such inelastic splittings in simple and natural ways.

3.2   Nucleon Scattering Rates

To compute the effective nucleon scattering rates $\sigma^0_{p,n}$ relevant for Eq. (2.2) mediated by a massive gauge boson, we concentrate exclusively on vector-vector (VV) interactions. Such VV interactions give rise to coherent *spin-independent* DM scattering off target nuclei [27]. Axial-axial (AA) interactions, on the other hand, produce an incoherent *spin-dependent* coupling to target nuclei. Mixed VA and AV interactions can also be neglected because they produce effective scattering cross sections suppressed by at least two powers of the DM velocity, which is on the order of $v \sim 10^{-3}$ in our galactic halo.

For fermionic IDM arising from couplings of the form given in Eq. (3.1), the effective nucleon cross section σ^0_n needed to compute the interaction rate Eq. (2.2) is identical to the cross section for a Dirac fermion to scatter off the nucleon. Up to small corrections, the effect of the inelasticity is completely accounted for by setting the lower velocity cutoff v_{min} in Eq. (2.1) to the expression given in Eq. (1.1). Starting with the Lagrangian for vector couplings of the SM quarks q and a Dirac fermion ψ to a massive Z' gauge boson (note we are using Z' here for generality – the next subsection will restrict attention to the Standard Model Z^0),

$$\mathscr{L} \supset -g\, g_V^q\, Z'_\mu\, \bar{q}\gamma^\mu q - g\, g_V^\psi\, Z'_\mu\, \bar{\psi}\gamma^\mu\psi, \tag{3.7}$$

the relevant effective nucleon-scattering cross section is [27]

$$\sigma^0_{p,n} = \frac{1}{\pi}\mu_{p,n}^2 \left(\frac{g}{M_{Z'}}\right)^4 (g_V^\psi g_V^{p,n})^2, \tag{3.8}$$

where $\mu_{p,n}$ is the reduced mass of the ψ-nucleon system, and

$$g_V^p = 2\,g_V^u + g_V^d, \qquad g_V^n = g_V^u + 2\,g_V^d. \tag{3.9}$$

The couplings f_p and f_n appearing in Eq. (2.2) coincide with g_V^p and g_V^n in the present case.

For complex scalar IDM, the effective nucleon scattering cross section required to evaluate the event rate in Eq. (2.1) is identical to the cross section for a single Dirac fermion of the same mass as the scalar to scatter off a nucleon. Again the effects of the inelasticity are accounted for by modifying the lower velocity cutoff v_{min} in Eq. (2.1). With the coupling of a complex scalar to a massive Z' given by

$$\mathscr{L} \supset -ig\,g_V^\phi\,Z'^\mu\,(\phi^*\partial_\mu\phi - \phi\partial_\mu\phi^*), \tag{3.10}$$

the effective nucleon scattering cross section is

$$\sigma_{p,n}^0 = \frac{1}{\pi}\,\mu_{p,n}^2\left(\frac{g}{M_{Z'}}\right)^4 (g_V^\phi g_V^{p,n})^2. \tag{3.11}$$

As for the fermionic case, we can identify $g_V^{p,n}$ with f_p and f_n appearing in Eq. (2.2).

3.3 $SU(2)_L$ Mediation

Perhaps the simplest possibility to mediate IDM scattering off nucleons is the Z^0 gauge boson of the SM. Note that the photon is not an option because we assume that the DM candidate is neutral and $W^\pm$ is not an option because the radiatively induced mass splitting between charged and neutral components of a multiplet scales as $\alpha_W M_W \sim 100\,\mathrm{MeV}$, which is much too large for IDM. A neutral particle that couples to the Z^0 necessarily carries hypercharge, so the simplest possibility is that dark matter is a doublet of $SU(2)_L$ with hypercharge $Y = 1/2$.

For a Dirac fermion or a complex scalar $SU(2)_L$ doublet with hypercharge $1/2$, the effective couplings for the neutral components are $g_V^{DM} = 1/2$, $g_V^p = 1/4 - \sin^2\theta_W$, and $g_V^n = -1/4$. Since $\sin^2\theta_W \simeq 0.24$, the neutron coupling is much larger than the proton coupling. The corresponding cross section is

$$\sigma_n^0 = \frac{G_F^2}{2\pi}\mu_n^2 \simeq 7.44 \times 10^{-39}\,cm^2. \tag{3.12}$$

To obtain this number, we assumed that the DM mass is much larger than that of the neutron so that $\mu_n \simeq m_n = 0.9396\,\mathrm{GeV}$.

In Figs. 4 and 5 we show fits to the DAMA modulated data along with constraints from CDMS II, CRESST-II, and ZEPLIN-III, for nucleon scattering mediated by Z^0-exchange and DM masses of 1080 GeV and 525 GeV, respectively. These particular masses were chosen because they are the values that lead to the correct thermal relic density for a Dirac fermion (1080 GeV) and a complex scalar doublet (525 GeV) [48].[7]

---

[7] Using micrOMEGAs v2.2 [55], we find slightly smaller central values for the preferred masses of 1080 GeV and 525 GeV as compared to Ref. [48], who obtain 1100 GeV and 540 GeV. However, these differences are within the margin of error and have a very small effect on the allowed region where the relic density scales roughly as $\Omega_{DM}h^2 \propto m_{DM}^2$.

It is intriguing that the inelastic cross section mediated by Z^0 exchange is very similar to the values preferred by our fit to DAMA. This coincidence of scales was observed in Ref. [13] in fitting the case of mixed sneutrino DM to the DAMA/NaI dataset. Here we observe that this persists even with more detailed fits to the energy spectrum and for more general doublet candidates.

The Z^0-mediated nucleon cross section is in fact a little bit too big assuming a local DM density of $\rho_{DM} = 0.3 \,\text{GeV}/cm^3$. However, there is a significant uncertainty in the local DM density and lowering its value to $\rho_{DM} = 0.15 \,\text{GeV}/cm^3$, which is also within the allowed range, leads to good agreement at the 90% confidence level for fermion doublet DM, and to marginal agreement for scalar doublet DM. Another possibility is that the dark matter has multiple components [56, 57, 58, 59], with the local density of the doublet component giving rise to the DAMA signal well below $0.3 \,\text{GeV}/cm^3$. The fermion or scalar doublet DM could also be heavier than 1080 GeV or 525 GeV and its density diluted by a late-time production of entropy, allowing for a larger cross section.

Let us also emphasize that the mass splitting terms in Eqs. (3.1) and (3.4) necessarily break $U(1)_Y$. However, such a mass term can be generated after electroweak symmetry breaking through operators involving the Higgs field [60]. The exact operator one needs then depends on the quantum numbers of the dark matter particle. For $SU(2)_L$-doublet dark matter with hypercharge $Y = 1/2$, we can introduce the gauge invariant operator

$$\mathscr{L} \supset -\frac{\lambda}{2}(\phi\phi hh + h.c.) \tag{3.13}$$

for a scalar, or

$$\mathscr{L} \supset -\frac{1}{2\Lambda}(\bar{\psi}^c\psi hh + h.c.) \tag{3.14}$$

for a fermion. In order to obtain a splitting $\delta \sim 100 \,\text{keV}$, we need $\lambda \sim (\delta/v)(m_\phi/v) \sim 10^{-6}$, or $\Lambda \sim (v^2/\delta) \sim 10^8 \,\text{GeV}$. While without further model structure (such as we will soon consider) these are somewhat awkward numbers, we emphasize that the values are technically natural.

Of course one can consider representations aside from an $SU(2)_L$ doublet. The next simplest possibility is to introduce a complex triplet of $SU(2)_L$ with hypercharge $Y = 1$. In order to split the states that couple to the Z^0, the triplet would require a higher-dimension operator $(T^{ij}h_i h_j)^2$ in order to be gauge invariant. For scalar DM, this operator should be suppressed by a scale $\Lambda^2 \sim (v^4/m_T\delta) \sim (10^5 \,\text{GeV})^2$, and for fermion DM it should be suppressed by a scale $\Lambda^3 \sim (v^4/\delta) \sim (3 \times 10^6 \,\text{GeV})^3$.

One can obviously keep considering larger representations of $SU(2)_L$, which will cause the scale suppressing the smallest gauge invariant splitting operator to decrease even further. In extensions to the Standard Model that solve the hierarchy problem, one might naturally expect to have operators suppressed by the TeV scale. Large enough representations of $SU(2)_L$ (*e.g.* a **5** or a **7**) may then naturally have the correct splitting. For a representation of dimension N, the DM mass needed to reproduce the right relic density, and hence the cross section needed for DAMA, increases roughly as $N^{3/2}$. On the other hand, the effective

scattering cross section σ_n^0 depends on the choice of hypercharge, and can scale between 1 and N^2. This means that thermal dark matter composed of a higher-dimensional representation can also agree with direct detection constraints, though the agreement can be better or worse according to the direct detection cross sections.

While it would be interesting to study the fits of larger representations of $SU(2)_L$ in more detail, we find it intriguing that the simplest possibility of an $SU(2)_L$ doublet works reasonably well for explaining the DAMA data. If one is to take this model of dark matter seriously, then, the main question is whether the numbers and scales cited above in Eqs. (3.13) and (3.14), though technically natural, have a reasonable origin in models. That is, suppose DAMA has indeed discovered dark matter. What would be a reasonable interpretation of this result? In Section 4, we will consider several possibilities for explaining the physical origin of these operators and their coefficients.

Figure 4: DAMA allowed region and constraints for scattering through Z^0-exchange for a fermion $SU(2)_L$ doublet with a mass of 1080 GeV, a value that yields the correct thermal relic density. We consider values of the DM escape velocity of $v_{esc} = 500\,km/s$ and $600\,km/s$ and local DM densities 0.15 GeV/cm^3 and 0.3 GeV/cm^3.

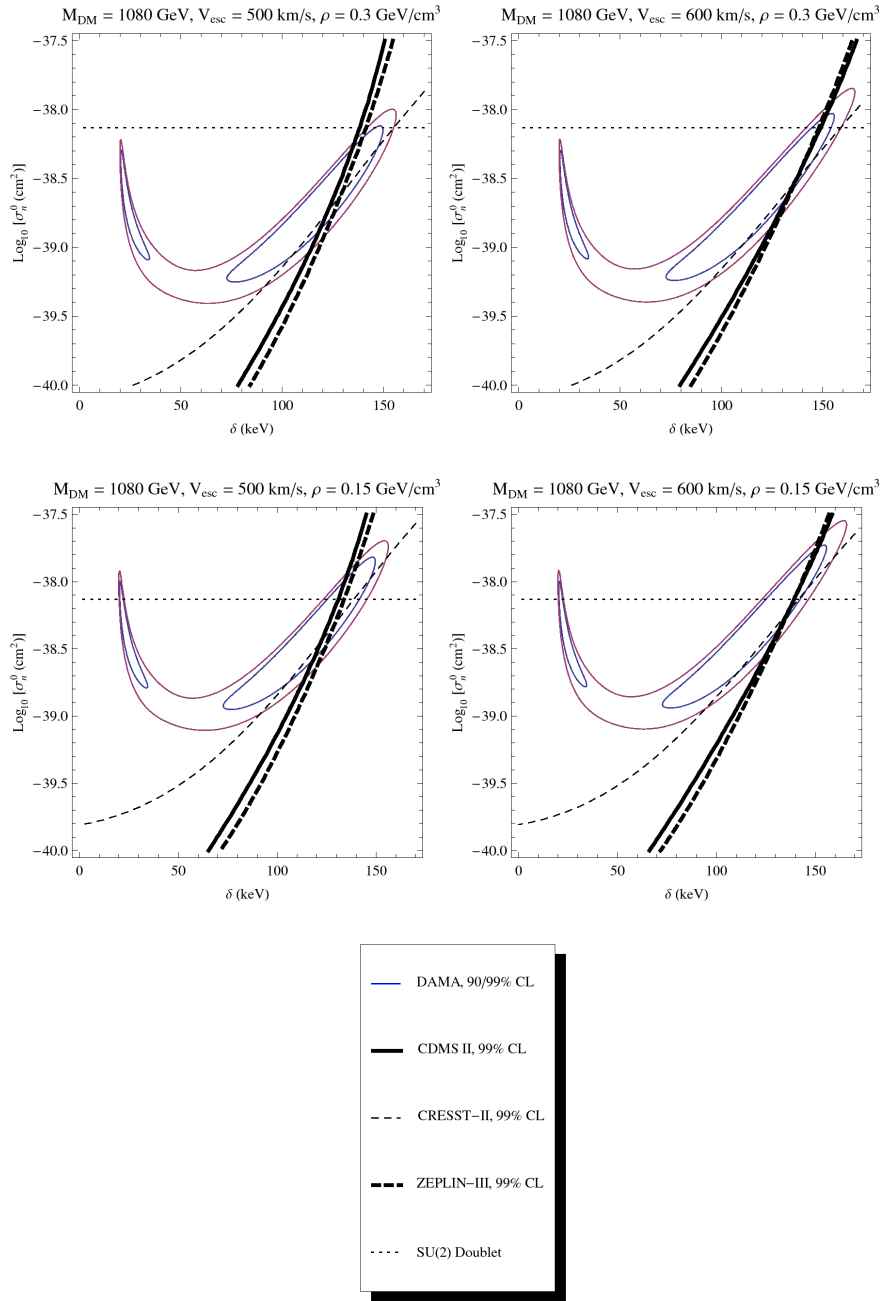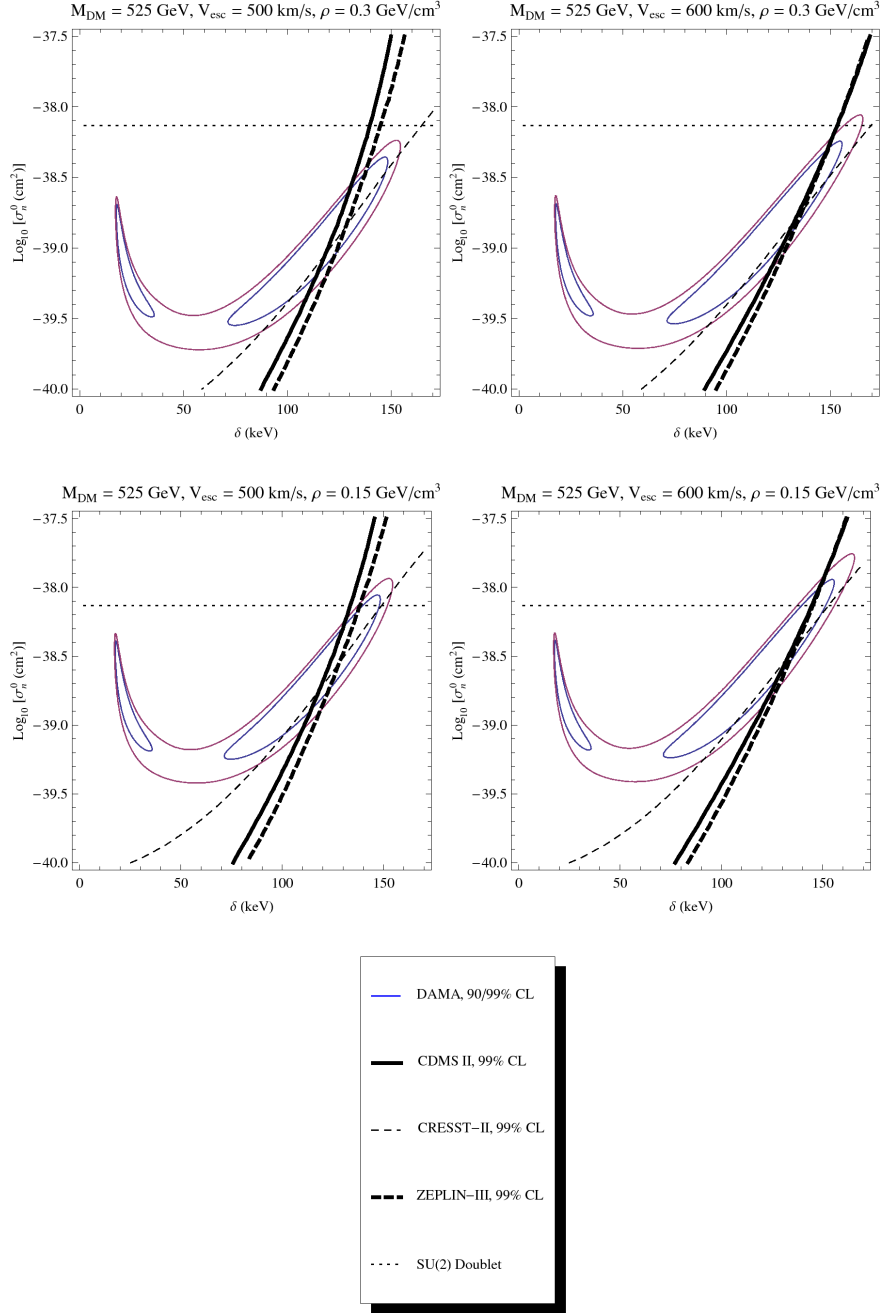Figure 5: DAMA allowed region and constraints for scattering through Z^0-exchange for a scalar $SU(2)_L$ doublet with a mass of 525 GeV, a value that yields the correct thermal relic density. We consider values of the DM escape velocity of $v_{esc} = 500\,km/s$ and $600\,km/s$ and local DM densities 0.15 GeV/cm^3 and 0.3 GeV/cm^3.

3.4 $U(1)_x$ Mediation

Inelastic DM scattering can also be mediated by a massive gauge boson not existing in the Standard Model. Two distinct possibilities that can yield the right cross sections are a heavy (TeV-scale) gauge boson with order unity couplings to Standard Model fields, and a light ($M_{Z'} \ll M_{Z^0}$) hidden gauge boson with highly suppressed couplings to the SM. If the hidden gauge symmetry is an Abelian $U(1)_x$, small couplings arise in a natural way from kinetic mixing with hypercharge. We consider here both the heavy and light exotic gauge boson cases, focusing on an Abelian $U(1)_x$ gauge symmetry for simplicity.

3.4.1 A Heavy Visible $U(1)_x$

A heavy $U(1)_x$ Z' gauge boson with order unity couplings to the SM can conflict with phenomenological bounds on the mass of this new state. Collider and other bounds place lower limits on the Z' mass, whereas a very heavy gauge boson generate a nuclear scattering cross section that is too small to account for DAMA, yielding some tension in this scenario.

Precision measurements at LEP imply that the bounds on lepton couplings for a given Z' mass are generally stronger than those for quarks. For example, a $(B - L)$ gauge boson would not satisfy phenomenological bounds and allow for a DAMA signal without unreasonably large couplings to the DM particle or an extremely small gauge coupling. Satisfying phenomenological constraints, even for a gauge coupling to the SM as small as $g_x \sim 0.4$, requires a gauge boson mass $M_{Z'} \gtrsim 2.5\,\mathrm{TeV}$. To achieve the DAMA signal would then require the effective coupling to dark matter to be greater than $g_x\, x_{DM} \gtrsim 10$, where x_{DM} is the dark matter charge. Lighter $(B - L)$ gauge bosons with perturbative couplings to the DM ($g_x\, x_{DM} \lesssim 1$) are possible at the expense of making the gauge coupling $g_x \lesssim 0.05$ while keeping $x_{DM} \gtrsim 20$. Such a hierarchy of charges seems contrived.

Models with smaller coupings to leptons relative to quarks and the DM are more reasonable. In Fig. 6 we show the values of the $U(1)_x$ charges of the leptons (x_E and x_L for e_R^c and L) and the DM particle (x_{DM}) for allowed points from a scan over heavy $U(1)_x$ models. These points satisfy both the phenomenological constraints on a heavy Abelian gauge boson and generate a reasonably large nuclear scattering cross section. We assume flavor-independent gauge charges (consistent with Yukawa couplings) for simplicity and to minimize flavor-violation, and take a two-Higgs doublet model for generality. Anomaly cancellation can be satisfied by adding exotic fermions. We have focused on charges such that $g_x\, x_i \leq 1$ to ensure weak coupling.

The phenomenological bounds we apply in generating Fig. 6 are the direct search bounds from the Tevatron in the di-lepton [61] and di-top [62] channels and the limits on contact interactions from LEP II [63]. In applying the Tevatron bounds, we assume the Z' decays entirely into SM final states. We do not explicitly compute the effects of the new $U(1)_x$ on precision electroweak observables, but demand that the $Z^0 - Z'$ mixing angle be less than $\theta_{mix} < 3 \times 10^{-3}$ [64, 65, 66, 67, 68, 69], which approximately captures the constraints from these observables [66]. In computing the mixing angle, we assume that $\tan\beta = 10$. For the
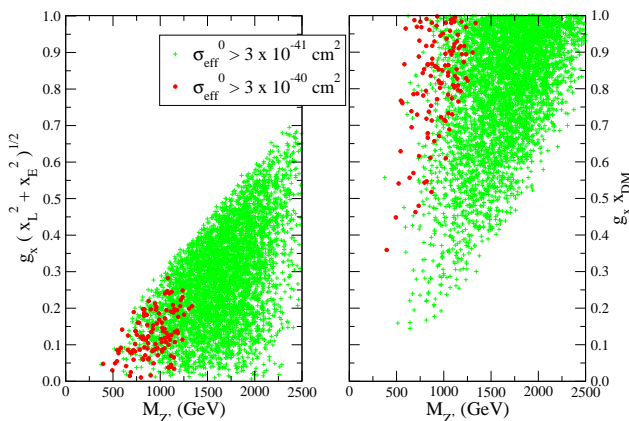
Figure 6: Values of the lepton and dark matter charges under $U(1)_x$ consistent with the phenomenological constraints listed in the text that also generate an adequately large value of the effective nucleon scattering cross section σ^0_{eff}, as a function of the Z' mass $M_{Z'}$. The charges of the quark and Higgs fields are also scanned over.

nucleon scattering cross section, we demand that the quantity

$$\sigma^0_{eff} \equiv \sigma^0_n \frac{[Z\,g^p_V + (A-Z)\,g^n_V]^2}{(g^n_V)^2 A^2} \tag{3.15}$$

be larger than $3 \times 10^{-41}\,cm^2$ or $3 \times 10^{-40}\,cm^2$. This definition and these lower limit values are motivated by our fits to IDM in Section 2, where we assumed $f_p = g^p_V = f_n = g^n_V$ in Eq. (2.2).

We conclude from Fig. 6 that a Z' with a mass in the range of 400 GeV to several TeV can generate an adequately large nucleon scattering cross section to account for DAMA while not running afoul of the existing bounds. Such a Z' must generally be somewhat leptophobic, and have significantly large couplings to quarks and the DM state. However, we note these couplings are so large that the corresponding gauge coupling generally encounters a Landau pole well below the GUT scale, even without including the effects of possible exotics required for anomaly cancelation (which would only make this problem worse). Thus, many popular $U(1)_x$ models such as $(B-L)$ and the exotic $U(1)$'s motivated by E_6 [70] do not work if a unification relation is imposed on the exotic gauge coupling. Furthermore, although this heavy Z' scenario is a possibility, the natural connection to the thermal relic abundance that was present with an electroweak cross section is in general lost.

3.4.2 A Light Hidden $U(1)_x$

A second possibility for an exotic Abelian gauge symmetry mediating IDM scattering at DAMA consists of a relatively light hidden $U(1)_x$ that couples only weakly to the SM. Very

small SM couplings arise naturally if the hidden sector couples to the SM through kinetic mixing of the $U(1)_x$ with hypercharge. A coupling [71]

$$\mathscr{L} \supset -\frac{\epsilon}{2} B_{\mu\nu} X^{\mu\nu}, \tag{3.16}$$

where $B_{\mu\nu}$ and $X_{\mu\nu}$ are the otherwise canonically normalized $U(1)_Y$ and $U(1)_x$ field strengths, can arise from loops of heavy states that are charged under both gauge groups. This leads to typical values of $\epsilon \simeq 10^{-4} - 10^{-2}$ [72]. Making a field redefinition to eliminate the kinetic mixing term, the SM matter fields acquire effective charges under the $U(1)_x$. If the DM states couple directly to the $U(1)_x$ but not the SM gauge groups, the exotic gauge boson can mediate DM scattering off nuclei.

We are interested in the case where the exotic Z' gauge boson is light, $M_{Z'} \ll M_Z$. In this limit the $U(1)_x$ can be treated as mixing with $U(1)_{em}$, and the induced charges are

$$\mathscr{L} \supset e \cos\theta_W \epsilon Q Z'_\mu \bar{f}\gamma^\mu f + \mathcal{O}(\epsilon M_{Z'}^2 / M_Z^2), \tag{3.17}$$

where f represents a SM fermion with electric charge Q. Since the light Z' couples to electric charge in the visible sector, it will mediate scattering of the DM only with protons. Applying Eq. (3.8) or Eq. (3.11), the corresponding cross section is

$$\sigma_p^0 = \left(\frac{g_x x_{DM}}{0.5}\right)^2 \left(\frac{\text{GeV}}{M_{Z'}}\right)^4 \left(\frac{\epsilon}{10^{-3}}\right)^2 (2.1 \times 10^{-36} \, cm^2), \tag{3.18}$$

where $g_x x_{DM}$ is the charge of the DM particle under the $U(1)_x$. Thus, for gauge boson masses of a few GeV and values of ϵ towards the lower end of the reasonable range, the DAMA signal can arise from IDM scattering off nuclei mediated by a hidden Z'.

Phenomenological bounds on a light hidden $U(1)_x$ have been studied in Refs. [66, 73, 74, 75, 76]. The strongest constraints on a hidden $U(1)_x$ gauge boson with mass of a few GeV, coupling to the SM through kinetic mixing with electromagnetism, comes from measurements of the magnetic dipole moments of the electron and muon. For masses larger than about a GeV, values of the kinetic mixing parameter ϵ less than 10^{-2} are acceptable [76].

If the mass of the dark matter particle is much larger than the mass of the light $U(1)_x$ gauge boson, a potential fermionic IDM candidate and its slightly heavier partner will both annihilate very efficiently into gauge boson pairs. The annihilation cross section for this process is [77]

$$\langle \sigma v \rangle_{VV} \simeq \frac{(g_x x_{DM})^4}{16\pi} \frac{1}{M_{DM}^2} \simeq \left(\frac{g_x x_{DM}}{0.5}\right)^4 \left(\frac{500 \, \text{GeV}}{M_{DM}}\right)^2 (5.8 \times 10^{-26} \, cm^3/s). \tag{3.19}$$

Note that this cross section scales as $\sim g_x^4 / M_{DM}^2$, just as for electroweak gauge boson exchange. For reference, the necessary thermal DM relic density is approximately $\Omega_{DM} h^2 \simeq 2\,(3 \times 10^{-27} cm^3/s)/\langle \sigma v \rangle$, where the additional factor of two accounts for the fact that two different states are annihilating [78, 79]. In addition, there are contributions to the annihilation cross sections from the s-channel exchange of $U(1)_x$ gauge bosons decaying into pairs of light matter fields in the $U(1)_x$ sector.

These contributions depend on the precise field content of the theory, but they will typically be on the same order as for annihilations into light gauge boson pairs. In general, the correct thermal relic density of a fermionic IDM state in this scenario will be obtained for a dark matter mass on the order of several hundreds of GeV. For a complex scalar IDM state, there is a moderate additional velocity suppression of the annihilation rate, and a somewhat lighter mass (but still on the order of a few hundred GeV) will yield the correct thermal relic density [73].

It follows from the discussion above and Eq. (3.18) that the we can choose parameters to give the correct thermal abundance while simultaneously accounting for the DAMA signal. Recall, however, that in the case of electroweak interactions this came out automatically for the known gauge boson masses and gauge coupling.

4   Models of Inelastic Dark Matter

Our guiding assumption in investigating candidates for IDM is that the interaction between the DM state and the target nucleus is mediated by a massive gauge boson. Though it is technically natural for the mass splitting operator coefficients to be small because they violate a global $U(1)_{DM}$ symmetry, the primary challenge is to generate a small inelastic mass splitting in a reasonable way. With this in mind, we introduce a $U(1)_{DM}$-breaking spurion ϕ. Depending on the relative charge of the dark matter field and ϕ, the mass splitting operator will be naturally suppressed by a factor $(\frac{<\phi>}{\Lambda})^n$. This operator could be used to generate a $\sim 100 \, \text{keV}$ splitting for a judicious choice of n and $<\phi>$.

This is not terribly satisfying, however, as it simply parameterizes our ignorance about how the symmetry is broken. We would also like to understand the physics underlying the inelastic splitting and, given that the masses generally hover around the electroweak scale, fit it together with possible solutions to the hierarchy problem. The goal of this section is to come up with simple models that can give rise to a splitting of the correct size in the context of a solution to the hierarchy problem without any large tuning of parameters. Of course, in the end aesthetic criteria are subjective, so we view this section as a compilation of interesting ways to generate splittings of the right size for fermions or scalars.

4.1   Models Mediated by the SM Z^0

As we saw in Section 3, dark matter charged under $SU(2)_L$ seems particularly promising because the Z^0-exchange cross section is roughly the correct size to account for the DAMA signal when one chooses a dark matter mass that gives the right thermal relic abundance. This is especially interesting for $SU(2)_L$ doublet dark matter, which is the simplest possible representation. However, the size of the mass splitting is then somewhat of a mystery, with scalar dark matter requiring the coefficient of the splitting operator Eq. (3.13) to be $\lambda \sim 10^{-6}$, and fermion dark matter requiring the splitting operator Eq. (3.14) to be suppressed by the mass scale $\Lambda \sim 10^8 \, \text{GeV}$. Both splittings are smaller than what one would naïvely expect

for an effective field theory valid below the TeV scale if $U(1)_{DM}$ were strongly broken.

One simple possibility is that the effects of $U(1)_{DM}$ breaking are sequestered in some way. This could happen, for example, if the splitting operators are generated by integrating out a singlet S through an operator DS^*h, where h is the SM Higgs field and D is the dark matter doublet. In this case, $U(1)_{DM}$ breaking could be communicated through the singlet. If the singlet is very heavy, or only couples weakly to the doublet D, the mass splitting is suppressed. Note that if there are multiple trilinear couplings DS^*h and DSh, we can simply call the linear combination that couples to the doublet S^* and define the $U(1)_{DM}$ symmetry so as to respect this trilinear coupling.

There are then two ways that $U(1)_{DM}$ breaking could be communicated. The first possibility is that most of the singlet mass is $U(1)_{DM}$ preserving, with a small $U(1)_{DM}$ breaking piece. For a scalar with the potential

$$\mathscr{L} \supset -m_S^2|S|^2 - \left(\frac{m_\delta^2}{2}S^2 + fDS^*h + h.c. \right), \tag{4.1}$$

integrating out the singlet generates the operator $\frac{f^2 m_\delta^2}{m_S^4}DDhh$. For a fermion with Lagrangian

$$\mathscr{L} \supset -m_S\bar{S}S - \left(\frac{m_\delta}{2}\bar{S}^cS + \lambda\bar{D}Sh + h.c. \right), \tag{4.2}$$

integrating out the singlet generates the operator $\frac{\lambda^2 m_\delta}{m_S^2}\bar{D}^cDhh$. If there is a natural hierarchy between m_δ and m_S, or if the couplings λ or f are naturally small, one could obtain a splitting of the correct size.

The second possibility is that the singlet has a very large $U(1)_{DM}$ breaking mass m_δ. This would, for example, be the only option if the singlet is a real scalar or a Majorana fermion. Integrating out the singlet would then generate the scalar operator $\frac{f^2}{m_\delta^2}DDhh$ or the fermion operator $\frac{\lambda^2}{m_\delta}\bar{D}^cDhh$. This is completely analogous to the way small neutrino masses are induced in the conventional seesaw mechanism.[8] A splitting of the right size could again be obtained for small couplings or if m_S is naturally identified with an intermediate scale.

Only a handful of concrete models exist for IDM whose nucleon scattering is mediated by the Z^0. Ref. [11] proposed a model of left-handed sneutrino dark matter in which the inelastic mass splitting is generated through mixing with a scalar singlet right-handed sneutrino. The $U(1)_{DM}$ violating (and lepton-number violating) mass arises through a SUSY breaking operator $\frac{1}{M_{Pl}^3}X^\dagger X^\dagger X N^\dagger N$, and the size of the splitting is naturally related to an intermediate scale. For related models, see Refs. [80, 81]. A second possibility for IDM are the Dirac neutralinos that arise in $U(1)_R$-symmetric SUSY scenarios [16, 17]. The small Majorana mass splitting would then be related to a small amount of $U(1)_R$ breaking.

We present below several other models for $SU(2)_L$ doublet IDM that make use of a singlet to communicate $U(1)_{DM}$ breaking. Two of these models are based on a warped extra

---

[8]In fact, it may be possible that the same right-handed neutrino scale enters both the neutrino mass and the dark matter splitting operators – this would require that the lepton doublets come with an additional suppression factor, but this may be natural in a model of flavor physics.

dimension [82], and illustrate some of the ways an inelastic splitting can emerge in this context. We also present a supersymmetric model.

4.1.1 Warped Fermion Model

We begin with a model of fermion $SU(2)_L$ doublet dark matter and attempt to explain how the scale of splitting $\delta \sim 100\,\text{keV}$ can emerge without any large hierarchy of input parameters. This requires an explanation for the scale suppressing the splitting operator Eq. (3.14), $\Lambda \sim 10^8\,\text{GeV}$, which could represent the mass of a singlet field that has been integrated out. One way that this intermediate scale mass could emerge naturally is if it is equal to the Planck scale times an exponential suppression factor. As we will see below, it is straightforward to realize this possibility in the context of a 5D Randall-Sundrum model [82], giving the added bonus of combining a natural dark matter model with a solution to the hierarchy problem. Our model is similar to the models of Refs. [83, 84], which realize the seesaw mechanism in warped geometry.

In particular, we consider AdS_5 compactified on $S_1/\mathbb{Z}_2$ with metric

$$ds^2 = e^{-2k|y|}\eta_{\mu\nu}dx^\mu dx^\nu - dy^2, \tag{4.3}$$

where $-\pi R \leq y \leq \pi R$. If the dark matter derives from a vector-like $SU(2)_L$ fermion doublet $D = (D_L, D_R)^T$ localized on the TeV brane, its mass is naturally of order the TeV scale. However, since we also expect the Higgs doublet to be localized to the TeV brane, we need to forbid the TeV brane localized operator $\frac{1}{\Lambda_{\text{TeV}}}\bar{D}^c Dhh$ which would generate too large of a splitting. We therefore impose a $U(1)_{DM}$ symmetry under which D is charged to forbid the splitting operator, and assume that this symmetry is broken only on the UV brane.

In order to communicate the breaking of $U(1)_{DM}$, we introduce a bulk fermion singlet $S = (S_L, S_R)^T$ with $(+,+)$ boundary conditions for S_L. We include a $U(1)_{DM}$-breaking Majorana mass on the UV brane, along with a $U(1)_{DM}$-preserving bulk mass. The singlet action is taken to be

$$S = \int d^4x \int dy \sqrt{-g}\left[i\bar{S}\gamma^M D_M S + ck\epsilon(y)\bar{S}S - \delta(y)\left(\frac{d_{UV}}{2}\bar{S}_L^c S_L + h.c.\right)\right.$$
$$\left. - \delta(y - \pi R)\left(\lambda \bar{D}_R S_L h + h.c.\right)\right] \tag{4.4}$$

where only the left-handed component of the singlet can have brane couplings because of the choice of boundary conditions. Here, $S^c = C\gamma^0 S^*$ where C is the 5D charge conjugation operator. The sign of the bulk mass parameter c has been chosen to agree with the convention that $c > 1/2$ localizes a zero mode towards the UV brane. Note that while the boundary singlet mass explicitly violates the $U(1)_{DM}$ symmetry, there remains an unbroken $\mathbb{Z}_2$ subgroup under which D and S are odd ensuring that the lightest of these fermions is stable.

To see the effect of the boundary terms on the fermion masses, it is easiest to first expand the singlet in a basis that diagonalizes the KK modes *without* the boundary terms. In this

basis, the communication of $U(1)_{DM}$ breaking is dominated by the chiral zero mode which picks up a large Majorana mass. Since the remaining modes acquire Dirac KK mass terms, we can truncate the KK tower while still capturing the dominant contribution. In particular, one can expand

$$S_{\substack{L\\R}}(x^\mu, y) = \frac{e^{2k|y|}}{\sqrt{2\pi R}} \sum_{n=0}^{\infty} S_{\substack{L\\R}}^n(x^\mu) f_{\substack{L\\R},n}(y), \tag{4.5}$$

where the wavefunctions $f_{\substack{L\\R},n}$ solve the bulk equations of motion

$$(\partial_y \pm ck) f_{\substack{L\\R},n}(y) = \mp m_n e^{k|y|} f_{\substack{R\\L},n}(y). \tag{4.6}$$

Imposing $(+,+)$ boundary conditions for S_L, the solutions are [85]

$$f_{\substack{L\\R},n}(y) = \frac{e^{k|y|/2}}{N_n} \left[J_{-c\mp\frac{1}{2}}\left(\frac{m_n}{k}e^{k|y|}\right) - \frac{J_{-c+\frac{1}{2}}\left(\frac{m_n}{k}e^{\pi kR}\right)}{Y_{-c+\frac{1}{2}}\left(\frac{m_n}{k}e^{\pi kR}\right)} Y_{-c\mp\frac{1}{2}}\left(\frac{m_n}{k}e^{k|y|}\right) \right]. \tag{4.7}$$

where the masses m_n can be determined from the condition that $f_{R,n}(0) = 0$, and the normalization factors are obtained from

$$\frac{1}{2\pi R} \int_{-\pi R}^{\pi R} dy \, e^{k|y|} \left(f_{L,m}^* f_{L,n} + f_{R,m}^* f_{R,n} \right) = \delta_{mn}. \tag{4.8}$$

In particular, there is a massless chiral zero mode with

$$f_{L,0}(y) = \sqrt{\frac{(2c-1)\pi kR}{1 - e^{-(2c-1)\pi kR}}} e^{-ck|y|}. \tag{4.9}$$

The other KK masses and normalization factors can be approximated for $m_n \ll k$ and $kR \gg 1$ as [85]

$$m_n \approx \left(n - \frac{c}{2}\right) \pi k e^{-\pi kR} \tag{4.10}$$

assuming $c < 1/2$, and

$$N_n \approx \sqrt{\frac{2}{\pi^2 \, R \, m_n}} e^{\pi kR/2}. \tag{4.11}$$

After performing this decomposition, the 4D fermion mass matrix is not yet diagonal due to the brane localized mass terms. The singlet mass matrix is

$$\mathscr{L} \supset -\frac{1}{2} \begin{pmatrix} \bar{S}_L^0 & \bar{S}_L^1 & \bar{S}_R^{1c} & \cdots \end{pmatrix} \begin{pmatrix} A_{00} & A_{01} & 0 & \cdots \\ A_{01} & A_{11} & m_1 & \cdots \\ 0 & m_1 & 0 & \cdots \\ \vdots & \vdots & \vdots & \end{pmatrix} \begin{pmatrix} S_L^{0c} \\ S_L^{1c} \\ S_R^1 \\ \vdots \end{pmatrix} + h.c. \tag{4.12}$$

26

where the Majorana masses A_{mn} are given in terms of the wavefunctions on the UV brane

$$A_{mn} \equiv \frac{d_{UV}}{2\pi R} f_{L,m}(0) f_{L,n}(0). \tag{4.13}$$

In particular, the zero mode picks up a mass

$$A_{00} = \frac{d_{UV} k(c - 1/2)}{1 - e^{-(2c-1)\pi k R}}. \tag{4.14}$$

The couplings to the canonically normalized doublet and Higgs field on the TeV brane are

$$\mathscr{L} \supset -\sum_{n=0}^{\infty} C_n \bar{D}_R S_L^n h + h.c. \tag{4.15}$$

where

$$C_n \equiv \frac{\lambda e^{\pi k R/2}}{\sqrt{2\pi R}} f_{L,n}(\pi R) \tag{4.16}$$

is determined from the wavefunction overlap on the TeV brane. Assuming that we choose c such that $A_{00} >> m_n$, we can to a good approximation simply integrate out the heavy chiral S_L^0 mode. This generates the splitting operator

$$\mathscr{L} \supset \frac{C_0^2}{2 A_{00}} \bar{D}_R^c D_R h h + h.c. \tag{4.17}$$

$$= \frac{\lambda^2}{2 d_{UV}} e^{-2(c-1/2)\pi k R} \bar{D}_R^c D_R h h + h.c. \tag{4.18}$$

Choosing the natural values $\lambda^2 \sim \frac{1}{M_{pl}}$ and $d_{UV} \sim 2$, we need $c \sim 0.13$ to obtain a mass splitting on the order of $\delta \sim 100\,\text{keV}$. It is straightforward to check that including the KK modes gives a negligible ($\sim 10^{-4}$) correction to these estimates (see Appendix A). This is due to the fact that, unlike the former zero mode, the states in the KK tower are mostly Dirac and are very poor at communicating $U(1)_{DM}$ breaking.

Arranging the model parameters to produce a mass splitting on the order of $\delta \sim 100\,\text{keV}$, our model has all the ingredients needed to account for the DAMA annual modulation result. The lightest stable fermion state is an almost pure $SU(2)_L$ doublet Majorana fermion with a slightly heaver inelastic partner, and is stable on account of the unbroken $\mathbb{Z}_2$ subgroup of $U(1)_{DM}$. If the corresponding fermion mass is $\sim 1.1\,\text{TeV}$, it will the yield the correct relic density from thermal freeze-out, in addition to the correct nucleon scattering cross section and mass splitting as was shown in Section 3.

4.1.2   Warped Scalar Model

We now turn to a model of scalar $SU(2)_L$ doublet dark matter. To sequester $U(1)_{DM}$ breaking we again consider a warped 5D setup with the metric of Eq. (4.3), and assume that

a complex scalar doublet $D = \frac{1}{\sqrt{2}}(D_R + iD_I)$ is localized to the TeV brane in addition to the Higgs field. As in the previous model, we need to forbid the TeV brane-localized operator $DDhh$, which would split the masses of D_R and D_I by $\sim \frac{v^2}{m_D}$ with an $O(1)$ coupling. We again assume a $U(1)_{DM}$ symmetry which is broken only on the UV brane, while preserving a $\mathbb{Z}_2$ subgroup to ensure the stability of the doublet DM.

In order to communicate this $U(1)_{DM}$ symmetry breaking to the DM doublet, we proceed as in the fermion model and introduce a bulk (scalar) singlet. Note that we cannot allow the doublet to directly couple to the UV symmetry breaking, even though a wavefunction localized to the TeV brane can be sufficiently suppressed in the UV, because the UV mass would then break hypercharge (since a neutral dark matter doublet must carry hypercharge) at too high a scale. Instead we assume the IR-brane-localized doublet mixes with a bulk singlet, as in the fermion model of the previous section.

The singlet can then couple in symmetry-breaking operators on the UV brane and communicate this breaking to the doublet on the TeV brane. However, we note a critical difference between 5D scalars and fermions – in general bulk scalars do not possess a zero mode. This means that the only option is to communicate $U(1)_{DM}$ breaking through singlet KK modes, which naturally peak away from the UV and tend to pick up small $U(1)_{DM}$-breaking masses (in addition to their $U(1)_{DM}$-preserving masses). Therefore this model does not suppress mass splitting via a seesaw mechanism. Instead, the real and imaginary components of the doublet will be split by their mixing to the split components of the bulk scalar KK modes.

In fact, bulk KK modes suppress the communication of $U(1)_{DM}$ symmetry breaking to the doublet extremely effectively – so much so that the effective UV scale cannot be much higher than $\sim 100 - 1000$ TeV or the $U(1)_{DM}$ breaking would effectively decouple and give too small a mass splitting to the dark matter candidate. In the context of an RS solution to the hierarchy problem, this requires a setup with either a third brane,[9] or an additional warped dimension such as was considered in Ref. [88]. Alternatively, one can simply treat the smaller warp factor as giving a solution to the flavor hierarchy problem, such as in the little RS scenario of Refs. [89, 90]. The model of this section can be thought of as a two-brane effective theory describing any of these situations, generated by integrating out physics above the effective UV scale.

We thus start by introducing a complex bulk singlet S with $(+, +)$ (Neumann) boundary conditions. In general, S has a bulk mass and two $U(1)_{DM}$-preserving brane mass terms, as well as a $U(1)_{DM}$-breaking mass term on the UV brane. To simplify the calculation we assume that the $U(1)_{DM}$-preserving brane mass terms are negligible. We consider the singlet action

$$
\begin{aligned}
S = & \int d^4x \int dy \sqrt{-g} \left[\partial_M S^* \partial^M S - m^2 S^* S - \delta(y) \left(\frac{m_{UV}}{2} S^2 + h.c. \right) \right. \\
& \left. - \delta(y - \pi R) \left(\lambda\, e^{2\pi kR}\, DS^* h + h.c. \right) \right],
\end{aligned}
\tag{4.19}
$$

---

[9]Detailed considerations of the three-brane setup, such as ensuring its stability, are beyond the scope of this work. Related references can be found in, *e.g.*, Refs. [86, 87].

where $m \equiv \sqrt{a}k$ is the $U(1)_{DM}$-preserving bulk mass of S, m_{UV} is the $U(1)_{DM}$-violating UV brane mass, and λ is the coupling to the dark matter field D. The exponential factor is because D and h are taken to be canonically normalized 4D fields, so $\lambda \sim \sqrt{k}$ has units of $\sqrt{\text{mass}}$.

The KK decomposition of S is

$$S(x^\mu, y) = \frac{1}{\sqrt{2\pi R}} \sum_n S^n(x^\mu) f_n(y), \tag{4.20}$$

where the functions $f_n(y)$ that solve the bulk equations of motion are [85]

$$f_n(y) = \frac{e^{2k|y|}}{N_n} \left[J_\alpha(\frac{m_n}{k} e^{k|y|}) + b_\alpha(m_n) Y_\alpha(\frac{m_n}{k} e^{k|y|}) \right]. \tag{4.21}$$

Here, $\alpha = \sqrt{4 + a}$, and the normalization factor N_n can be approximated in the limit $m_n << k$ and $kR >> 1$ as

$$N_n \approx \sqrt{\frac{1}{\pi^2 \, R \, m_n}} e^{\pi k R/2}. \tag{4.22}$$

The masses m_n and the functions b_α are determined from the boundary conditions. In the $U(1)_{DM}$-symmetric limit ($m_{UV} = 0$), the boundary conditions of S_R and S_I are identical, so there is a pair of degenerate states at each KK level. When $U(1)_{DM}$ is broken ($m_{UV} \neq 0$), S_R and S_I have different boundary conditions and the resulting KK masses are split.

In the presence of the $U(1)_{DM}$-violating mass, variation of the boundary action determines the boundary conditions to be

$$\partial_y S_{R \atop I} \mp m_{UV} S_{R \atop I} = 0|_{y=0} \tag{4.23}$$
$$\partial_y S_{R \atop I} = 0|_{y=\pi R}.$$

It is straightforward to solve numerically for the KK mode mass splitting in the presence of these boundary conditions. This mass splitting in the singlet sector is then communicated to the DM doublet through the couplings on the TeV brane.

It is easier however to proceed as in the last section and first expand the KK states in the basis without the splitting, treating the $U(1)_{DM}$-violating mass as a perturbation. Imposing the simpler boundary conditions $\partial_y S = 0|_{y=0,\pi R}$ leads to the two conditions

$$b_\alpha(m_n) = -\frac{2J_\alpha(\frac{m_n}{k}) + \frac{m_n}{k} J'_\alpha(\frac{m_n}{k})}{2Y_\alpha(\frac{m_n}{k}) + \frac{m_n}{k} Y'_\alpha(\frac{m_n}{k})} \tag{4.24}$$

$$= -\frac{2J_\alpha(\frac{m_n}{k} e^{\pi k R}) + \frac{m_n}{k} e^{\pi k R} J'_\alpha(\frac{m_n}{k} e^{\pi k R})}{2Y_\alpha(\frac{m_n}{k} e^{\pi k R}) + \frac{m_n}{k} e^{\pi k R} Y'_\alpha(\frac{m_n}{k} e^{\pi k R})} \tag{4.25}$$

which yield the approximate KK spectrum in the limits $m_n << k$ and $kR >> 1$ [85],

$$m_n \approx \left(n + \frac{\alpha}{2} - \frac{3}{4} \right) \pi k \, e^{-\pi k R}. \tag{4.26}$$

In this basis, the masses in the singlet sector can be written as

$$
\mathscr{L} \supset -\frac{1}{2} \begin{pmatrix} S_R^1 & S_R^2 & \dots \end{pmatrix} \begin{pmatrix} m_1^2 + \Delta_{11}^2 & \Delta_{12}^2 & \dots \\ \Delta_{21}^2 & m_2^2 + \Delta_{22}^2 & \dots \\ \vdots & \vdots & \end{pmatrix} \begin{pmatrix} S_R^1 \\ S_R^2 \\ \vdots \end{pmatrix}
$$
$$
-\frac{1}{2} \begin{pmatrix} S_I^1 & S_I^2 & \dots \end{pmatrix} \begin{pmatrix} m_1^2 - \Delta_{11}^2 & -\Delta_{12}^2 & \dots \\ -\Delta_{21}^2 & m_2^2 - \Delta_{22}^2 & \dots \\ \vdots & \vdots & \end{pmatrix} \begin{pmatrix} S_I^1 \\ S_I^2 \\ \vdots \end{pmatrix} \qquad (4.27)
$$

where

$$
\Delta_{mn}^2 \equiv \frac{m_{UV}}{2\pi R} f_m(0) f_n(0). \qquad (4.28)
$$

The mass splitting in the singlet sector at each KK level is then determined by the difference in the eigenvalues of these two mass matrices. As long as we choose parameters such that $\Delta_{mn} << m_n$, the mixing is small and the eigenvalues are simply $m_n^2 \pm \Delta_{nn}^2$ up to $O(\frac{\Delta^4}{m^2})$ corrections. Expanding the wavefunction profiles in Eq. (4.21) for $m_n << k$ at $y = 0$, the mass splitting at the nth KK level is then approximately

$$
\Delta m_n \approx \frac{\Delta_{nn}^2}{m_n}
$$
$$
\approx \left(\frac{m_n}{k}\right)^{2\alpha} \left[\frac{\pi \, e^{-\pi kR} \, m_{UV}}{2^{2\alpha-1} \, \Gamma(\alpha)^2 \, (\alpha-2)^2}\right]. \qquad (4.29)
$$

The mass splitting in the singlet sector is transmitted to the DM doublet through their coupling on the TeV brane. After the Higgs acquires a VEV, the mass matrix is

$$
\mathscr{L} \supset -\frac{1}{2} \begin{pmatrix} D_R & D_I & S_R^1 & S_I^1 & \dots \end{pmatrix} \begin{pmatrix} m_D^2 & 0 & C_1 v & 0 & \dots \\ 0 & m_D^2 & 0 & C_1 v & \dots \\ C_1 v & 0 & m_1^2 + \Delta_{11}^2 & 0 & \dots \\ 0 & C_1 v & 0 & m_1^2 - \Delta_{11}^2 & \dots \\ \vdots & \vdots & \vdots & \vdots & \end{pmatrix} \begin{pmatrix} D_R \\ D_I \\ S_R^1 \\ S_I^1 \\ \vdots \end{pmatrix} (4.30)
$$

where

$$
C_n \equiv \frac{\lambda e^{-2\pi kR}}{\sqrt{2\pi R}} f_n(\pi R). \qquad (4.31)
$$

It is straightforward to diagonalize this mass matrix at a given level of truncation of the KK tower. For example, including just the first KK state leads to a mass squared splitting to leading order in Δ_{11} of

$$
\Delta m_D^2 \approx \Delta_{11}^2 \left[1 - \frac{|m_1^2 - m_D^2|}{\sqrt{(m_1^2 - m_D^2)^2 + 4C_1^2 v^2}}\right]. \qquad (4.32)
$$

Note that this goes to zero if either the UV brane mass or TeV brane coupling turns off, just as one would expect. We can further expand this for small $v << m_n$, and write the contribution from the n$^\text{th}$ KK level more generally as

$$\Delta m_D \approx \Delta m_n \frac{C_n^2 v^2}{m_D m_n^3} \left(1 + \frac{2m_D^2}{m_n^2} \right), \qquad (4.33)$$

where Δm_n is the singlet mass splitting at the nth KK level, given approximately in Eq. (4.29). Choosing the values $k \sim 500\,\text{TeV}$, $R \sim 2.1/k$, $m_{UV} \sim 2k$, $a \sim 0.1$, $\lambda \sim 2.5\sqrt{k}$, and $m_D \sim 525\,\text{GeV}$, for example, gives a contribution to the DM mass splitting from the first KK mode of $\sim 5\,\text{keV}$.[10] Note that a splitting in the singlet sector that is not too small requires the warp factor kR not be too large.

However, when trying to sum these KK contributions, the sum apparently diverges. This is counter-intuitive, since we would expect heavy modes to decouple. Here we might expect this decoupling to happen since the contribution to the splitting appears to be smaller for heavier KK modes due to the $\sim 1/n^3$ suppression in Eq. (4.33). However, this is compensated for by the fact that the singlet splitting Δm_n is increasing for higher KK modes due to a larger UV brane overlap, and scales roughly as $\sim n^{2\alpha} \gtrsim n^4$.

The issue then is the behavior of C_n for higher KK modes. In the naïve limit of an infinitely thin brane, the higher KK modes would appear to couple to the TeV brane with roughly equal strength, and the magnitude of C_n would not significantly change as one increases n. This behavior was seen, e.g., in Refs. [91, 92], where the IR brane coupling of KK SM gauge fields was studied and found to be universal. This would lead to a contribution to the DM mass splitting that increases approximately linearly with n for small values of the bulk mass a.

However, this result is unphysical since it does not take into account the thickness of the IR brane, $\Delta \sim \Lambda^{-1}$, where Λ is the 5D cutoff scale and the thickness is given in y-coordinate space. We expect $\Lambda \sim (10-100)\,k$ based on naïve dimensional analysis. Note that the physical thickness of the brane at $y \simeq \pi R$ is redshifted to $\Delta_{phys} \sim \Lambda^{-1} e^{\pi k R}$. The effective 4D coupling C_n^{eff} is then better approximated by integrating the wavefunctions over this thickness. While not terribly important for lower KK modes, higher KK modes rapidly oscillate over this region and the effective coupling is suppressed due to a cancelation between opposite phases.

While the exact numerics depend on the details of the Higgs and DM doublet wavefunction profiles over the brane thickness, we can understand this decoupling by assuming the "flat" profiles

$$f_{h,D}(y) \simeq \frac{1}{\sqrt{\Delta}} e^{ky}, \qquad (4.34)$$

and concretely taking $\Delta^{-1} \sim 10\,k$. The effective coupling C_n^{eff} is then given by

$$C_n^{eff} \simeq \frac{\lambda}{\sqrt{2\pi R}} \frac{1}{\Delta} \int_{\pi R - \frac{\Delta}{2}}^{\pi R + \frac{\Delta}{2}} dy\, e^{-2ky}\, f_n(y). \qquad (4.35)$$

---

[10]Note that while $kR \sim 2.1$ is not much larger than 1 as was assumed in some of the approximations above, we find that the analytical formulae still give a reasonable approximation to the full numerical results.

With these choices, only the first $\sim \Lambda/k \sim 10$ KK modes make a significant contribution to the DM mass splitting. Taking the same parameters as before, we obtain a mass splitting of $\sim 70\,\text{keV}$ when summing over the first 10 KK modes. Note that this decoupling behavior itself is quite robust in that it will happen for any reasonable choice of Higgs and DM doublet profiles.

For higher values of n, the integrand in Eq. (4.35) is rapidly oscillating over the brane thickness Δ. This happens when the KK modes have enough 5D momentum such that many wavelengths λ_n fit inside the physical thickness of the brane. We then expect a phase cancelation up to terms suppressed by about $\sim \lambda_n/\Delta_{phys} \sim 1/n$ (see Appendix B for a more detailed derivation). For small bulk mass a, Δm_n in Eq. (4.29) scales roughly as $\sim n^4$, so the mass splitting in Eq. (4.33) now scales as $\sim 1/n$. Summing the contributions from these higher KK modes up to $n \simeq \frac{\Lambda}{k} e^{\pi k R}$ (corresponding to modes with momentum around the 5D cutoff scale) then gives an additional contribution which is enhanced by $\sim \log(e^{\pi k R}) \sim 6$ relative to the contribution from a single lower mode. Estimating the overall amplitude as $\sim 1/10$ of the sum of the first 10 modes, these higher KK modes can then give an $O(1)$ correction to the mass splitting, and one can obtain a splitting of the desired size.

4.1.3   A Supersymmetric Candidate

The mechanism described above for generating a splitting, namely mixing the DM doublet with a singlet that has a $U(1)_{DM}$-breaking mass, can apply in other contexts as well. We next consider the application of this mechanism in the context of low-energy supersymmetry. In this case, a natural small suppression can arise for example in large $\tan\beta$ scenarios when mixing the singlet with the doublet dark matter candidate through the VEV of H_d.

An example of a model that exploits this suppression consists of the MSSM augmented by a vector pair of $SU(2)_L$ doublet chiral superfields D and D^c with $Y = \pm 1/2$. Hypercharge and holomorphy then allow the superpotential operator DD^c, but not DD or $D^c D^c$, and an accidental $U(1)_{DM}$ global symmetry can arise. This symmetry must be broken to generate an inelastic splitting. To do so, we gauge a related $U(1)_z$ symmetry and break it by Higgsing. A simple superpotential that realizes the above symmetries is

$$W \supset \lambda\, N\, H_u \cdot H_d + \lambda'\, S\, H_d \cdot D + \frac{\xi}{2}\, N\, S^2 + \zeta\, N\, D D^c. \qquad (4.36)$$

Here, N and S are SM singlets that carry non-zero charges under the gauged $U(1)_z$ group.

If the N field develops a VEV induced by supersymmetry breaking soft terms, $N \to \langle N \rangle \sim$ TeV, a supersymmetric mass for S will be generated.[11] To get an approximate picture of what this does to the masses of the fermions in the model, we can integrate out the S superfield in the supersymmetric limit. This yields

$$W_{eff} \supset \lambda\, \langle N \rangle\, H_u \cdot H_d + \zeta\, \langle N \rangle\, D D^c - \frac{\lambda'^2}{2\xi\, \langle N \rangle}\, (H_d \cdot D)^2. \qquad (4.37)$$

---

[11]The size of the N VEV can be set by SUSY breaking so that it is naturally on the order of a TeV. The N scalar will get a mass upon expanding the scalar potential, while the N fermion will develop a mass by mixing with the $U(1)_z$ gaugino.

The last term is the desired mass splitting operator. It receives a suppression from large $\tan\beta$, our choice that $\lambda' < 1$, and from an assumed small hierarchy between $\langle N \rangle$ and the electroweak scale. A more careful analysis of mixing in the SM-neutral fermion sector after symmetry breaking shows that the fermion mass eigenstates consist of an almost pure singlet and a nearly degenerate pair of Majorana states that derive almost entirely from the doublets. The resulting SM-neutral fermion masses are

$$M_{d_{\frac{1}{2}}} = \zeta\,\langle N \rangle + \delta_{\pm}, \qquad M_s = \xi\,\langle N \rangle + \delta_{+} - \delta_{-}, \tag{4.38}$$

with

$$\delta_{\pm} \simeq \pm \frac{\lambda'^2 v_d^2}{2M_s}\left(1 \pm \frac{M_d}{M_s}\right)^{-1}. \tag{4.39}$$

Taking $\tan\beta = 30$, $M_s = 3000$ GeV, $M_d = 1000$ GeV, and $\lambda' = 0.1$, we obtain a mass splitting of $\delta_{+} - \delta_{-} \simeq 130$ keV.

The neutral fermion components of D and D^c can therefore yield IDM provided these fields are stable. An unbroken $\mathbb{Z}_2$ discrete symmetry is the minimal possibility to ensure this. If this symmetry is R-parity, D and D^c as well as the N and S superfields must all be even. On the other hand, with a new $\mathbb{Z}_2$ it is possible for D, D^c, and S to be odd, with N and the Higgs fields even. The inclusion of such a new discrete symmetry is well-motivated in gauge-mediated models with a light gravitino.

The form of the superpotential in Eq. (4.36) can be enforced by the $U(1)_z$ charges

$$[S]_z = z_s, \quad [N]_z = -2z_s, \quad [D]_z = z_d, \quad [D^c]_z = 2z_s - z_d, \tag{4.40}$$
$$[H_d]_z = -z_s - z_d, \quad [H_u]_z = 3z_s + z_d.$$

With these charges, the dangerous operator $[H_u \cdot d^c]_z = 5z_s$ is forbidden provided $z_s \neq 0$, as is the bare μ term operator $[H_u \cdot H_d]_z = 2z_s$. Note also that if $z_d = z_s$, a $\mathbb{Z}_2$ that stabilizes both D and D^c arises automatically as an unbroken discrete subgroup of the $U(1)_z$ gauge symmetry. As it stands, this theory has mixed $SU(2)_L^2 \times U(1)_z$, $U(1)_Y^2 \times U(1)_z$, and $U(1)_z^2 \times U(1)_Y$ anomalies when $z_s \neq 0$, implying that SM-charged exotics must also be present in the theory. In fact, such exotics are necessary in any MSSM gauge extension that forbids a bare μ-term [96, 97]. These exotics need not interfere with the dynamics discussed here.

It is more challenging to obtain an acceptable scalar inelastic dark matter splitting from this model. The scalar components of D and D^c will be stable if these superfields (and S) are odd under R-parity or if we impose a new $\mathbb{Z}_2$ discrete symmetry. In the latter case, it is necessary to tune the soft masses such that the fermion components of D and D^c are heavier than the scalars. At the supersymmetric level, a scalar mass splitting arises from the F-term potential for H_d derived from the effective superpotential of Eq. (4.37)

$$V_F \supset \left| \frac{\lambda'^2}{\xi\,\langle N \rangle} H_d \cdot \tilde{D}\,\tilde{D} + \mu_{eff}\, H_u \right|^2 \tag{4.41}$$
$$\supset M_d \left(\frac{\lambda'^2 \mu_{eff}\, v_u v_d}{M_d\, M_s} \right) \tilde{D}\tilde{D} + h.c.,$$

with M_d and M_s as in Eq. (4.38), and $\mu_{eff} = \lambda \langle N \rangle$. Relative to the fermion splitting of Eq. (4.39), this operator is suppressed by only a single power of $\cos \beta \sim 1/\tan \beta$ at large $\tan \beta$. If generic soft supersymmetry breaking operators are also included, there arises a further scalar mass splitting with no $\cos \beta$ suppression at all. This contribution can be thought of as coming from an operator of the form

$$\mathscr{L}_{eff} \supset -M_d \left(\frac{\lambda'^2 A_\xi \, \mu_{eff}^2 v_u^2}{M_d \, M_s^3} \right) \tilde{D}\tilde{D} + h.c., \tag{4.42}$$

where A_ξ is the trilinear soft parameter corresponding to the $\xi N S^2$ superpotential operator. Numerically, we find that the operators of Eq. (4.41) and (4.42) produce too large of an inelastic scalar mass splitting unless $\lambda' \lesssim 0.01$ and there is an additional small hierarchy between μ_{eff}, A_ξ and M_d, M_s. Note that even when the scalar splitting is too large, the radiative corrections to the fermion mass splitting are still safely small.

Scattering off nuclei by the IDM candidates that arise in this model will be mediated primarily by the SM Z^0. The massive $U(1)_z$ gauge boson can also contribute to nuclear scattering, but the effect will be suppressed by its larger mass. If the new states in the $U(1)_z$ sector are somewhat heavier than the IDM candidate, the thermal relic density will be determined primarily by electroweak interactions, and our estimates from Section 3 for the relic density carry through. An interesting additional possibility arises when the doublet IDM state is stabilized by a new $\mathbb{Z}_2$ symmetry, rather than R-parity. In this case, the lightest superpartner will provide a second contribution to the dark matter. Such multi-component DM scenarios have been considered in a number of recent works [56, 57, 58, 59]. As long as any additional DM component has a small scattering cross section off nuclei, it will not ruin the IDM explanation for the DAMA signal provided the IDM component makes up a significant fraction of the DM relic abundance.

4.2 Models Mediated by an Exotic Z' Gauge Boson

In Section 3 we showed that the DAMA signal can arise from the scattering of IDM off iodine nuclei mediated by an exotic $U(1)_x$ gauge boson. We distinguish two possibilities for such a gauge boson, one in which it is heavier than the SM Z^0 and couples directly to the SM and the other in which it is much lighter than the Z^0 and couples only weakly to the visible sector, such as through a small kinetic mixing with electromagnetism. We construct here models for IDM that realize both possibilities, though we will see the latter involves mass scales that are more contrived.

4.2.1 Heavy $U(1)_x$ Models

The Z^0-mediated candidates for IDM presented above can all be adapted to models in which the scattering off nuclei is mediated by the exchange of a heavy $U(1)_x$ gauge boson. In each case, the $SU(2)_L$ doublet states in our previous models are replaced by a pair of states with vector-like charges under a $U(1)_x$ gauge symmetry. For the analog of our SUSY

model, the $U(1)_x$ gauge symmetry should be broken by a pair of fields such that they obtain hierarchically different expectation values from the dynamics of the potential.

In contrast to the Z^0-mediated models presented above, however, the thermal relic density in heavy $U(1)_x$ models is more model dependent. If the DM particle is lighter than the exotic gauge boson, it will no longer annihilate into gauge boson pairs. Annihilation into matter fields from s-channel exchange of heavy gauge bosons is suppressed by the larger gauge boson mass (and depends on the number of channels into which the gauge boson can decay). This can allow for thermal dark matter that is somewhat lighter than in the doublet case, which can provide a better IDM fit to the direct detection data.

4.2.2 A Light $U(1)_x$ Model

IDM scattering at DAMA can also be mediated by a new light gauge boson that couples directly to the DM, but only very weakly to the visible SM sector. This can arise from an exotic $U(1)_x$ gauge boson with a mass on the order of a few GeV that has a kinetic mixing with electromagnetism on the order of $\epsilon \sim 10^{-4} - 10^{-3}$. We describe a minimal supersymmetric realization of such a scenario in this section. However, in this scenario and others like it, new mass scales must be put in by hand. Thus, we find this scenario less compelling from the point of view of naturalness (not technical naturalness) but permissible so we include it as a logical possibility.

Supersymmetry affords a natural setting for light exotic gauge bosons in sectors that are somewhat shielded from the source of supersymmetry breaking. The smaller supersymmetry breaking soft terms in the hidden sector can then induce symmetry breaking in that sector at a scale that is parametrically smaller than the electroweak scale. However, the minimal model we describe below also contains supersymmetric mass scales whose origin requires further explanation.

Our IDM model contains two pairs of SM-singlet chiral superfields, a and a^c along with H and H^c, such that each pair has vector-like charges under a new $U(1)_x$ gauge symmetry. The model also contains a pure singlet, S, uncharged under both the SM and $U(1)_x$. Both a and a^c as well as S are assumed to be odd under an exact unbroken $\mathbb{Z}_2$ symmetry. We take the superpotential to be

$$W \supset \mu' H H^c + M_a a a^c + \frac{1}{2} M_s S^2 + \lambda_1 S a^c H + \lambda_2 S a H^c, \qquad (4.43)$$

where we assume $M_a \sim M_s \sim$ TeV and $\mu' \sim$ GeV. We assume further that the fields in this sector are shielded from supersymmetry breaking relative to the MSSM sector. This can hold if supersymmetry breaking is mediated to the visible sector by gauge mediation through messengers charged only under the MSSM gauge group, for example.

In the context of gauge mediation, kinetic mixing with hypercharge then induces effective charges for the gauge messengers under the $U(1)_x$ symmetry that are suppressed by the mixing parameter. The resulting soft scalar masses in the $U(1)_x$ sector are thus on the order of $m_x^2 \sim (g_x/g')^2 \epsilon^2 m_{E^c}^2$, where $\epsilon \sim 10^{-4} - 10^{-3}$ is the kinetic mixing parameter and $m_{E^c}^2$ is

the soft scalar mass of the right-handed selectron [98, 99, 59, 100]. Upon running down to lower energies, the scalar soft masses for H and H^c can be induced to run negative by way of large Yukawa couplings, generating VEVs for these fields on the order of a GeV [59, 100]. The H and H^c scalars can also be destabilized at the origin by the contribution to the $U(1)_x$ D-term potential from the MSSM Higgs fields, which obtain small $U(1)_x$ charges from gauge kinetic mixing. The hidden sector VEVs generated in this way will be on the order of $\sqrt{\epsilon}\, v$. If the scale of gauge mediation is relatively high, the $U(1)_x$ sector can also receive additional small soft breaking contributions from gravity mediation [15, 101].

Integrating out S generates the effective superpotential

$$W_{eff} \supset \mu' H H^c + M_a\, a\, a^c - \frac{\lambda_1^2}{2M_s}\, (a^c H)^2 - \frac{\lambda_2^2}{2M_s}\, (aH^c)^2 - \frac{\lambda_1 \lambda_2}{M_s}(a^c H)(aH^c). \qquad (4.44)$$

From this we obtain the fermion mass splitting

$$\delta = \frac{\lambda_1^2 \langle H \rangle^2 + \lambda_2^2 \langle H^c \rangle^2}{M_s} = 2\lambda^2 \left(\frac{\langle H \rangle}{\mathrm{GeV}}\right)^2 \left(\frac{\mathrm{TeV}}{M_s}\right)\ \mathrm{MeV}, \qquad (4.45)$$

where in the second equality above we have assumed $\lambda_1 = \lambda_2 = \lambda$ and $\langle H \rangle = \langle H^c \rangle$. With a small amount of suppression from the couplings, this is of the right size for IDM. From the F terms of H and H^c we also get scalar splittings

$$\begin{aligned} V_F \quad \supset \quad & -\mu' \frac{\lambda_1^2}{2M_s}\, H^\dagger H^c\, \tilde{a}^2 - \mu' \frac{\lambda_2^2}{2M_s}\, H^{c\dagger} H\, \tilde{a}^{c2} \\ & -\frac{\lambda_1^2}{M_s}\, M_a\, (H^c)^2\, \tilde{a}\, \tilde{a}^{c*} - \frac{\lambda_2^2}{M_s}\, M_a\, (H)^2\, \tilde{a}^c\, \tilde{a}^* + h.c.. \end{aligned} \qquad (4.46)$$

The first two terms here are subleading, while the second two generate scalar mass splittings of the right size with a small amount of additional suppression from the couplings $\lambda_{1,2}$. Note that either the fermion or the scalar can be the dark matter state, whichever is lighter, depending on the soft terms.

While the superpotential of Eq. (4.43) is technically natural, this model does not give an explanation for why M_a and M_s are so much larger than μ'. A value of μ' on the order of a GeV can perhaps arise naturally from an NMSSM-like extension of the Higgs sector in this model, as in Refs. [59, 100]. It could also arise from a Giudice-Masiero [102] coupling to supergravity in high-scale gauge mediation [101]. The larger masses M_a and M_s could also potentially be generated by an NMSSM-like extension coupling to $a^{(c)}$ and S [100], although this possibility would be more complicated.

The model described above is similar to the one presented in Refs. [15, 101]. There, the larger mass is also put in by hand, the smaller mass is related to the breakdown of a non-Abelian gauge symmetry near a GeV, and the inelastic mass splitting arises radiatively from gauge boson loops. However, because this mechanism for inelastic splitting works only with a non-Abelian gauge group, the construction also requires a higher-dimensional operator in order to generate kinetic mixing with hypercharge, $Tr(\mathcal{O}^{(n)\,a}\, W_{\mu\nu}^a)\, B^{\mu\nu}/M^n$, where $\mathcal{O}^{(n)\,a}$ is a chiral adjoint operator under the exotic gauge group of dimension n. It requires additional model ingredients to explain the origin of the scale M which cannot be too large in order to obtain a large-enough mixing angle.

5 Conclusions

In this paper we have considered the possibility that DAMA is a true discovery of dark matter, and investigated the properties a theory of dark matter needs to have in order to account for the data. We have shown that inelastic dark matter is consistent with the findings of DAMA as well as other direct detection experiments and seems to provide a better account for the sum of this data than other proposed explanations such as light elastic dark matter or dark matter scattering off detector electrons. Extending the study of Ref. [14], we find that heavier inelastic dark matter can give a reasonable fit to the data, particularly for lower values of the galactic DM escape velocity.

An intriguing additional observation is that if the inelastic dark matter candidate is an electroweak doublet, it can simultaneously have the correct thermal relic abundance and a nucleon scattering cross section mediated by the SM Z^0 in the range consistent with DAMA and other experiments. For a scalar doublet, this occurs when its mass is close to 525 GeV, while for a fermion doublet the mass should be about 1080 GeV. This makes electroweak-doublet inelastic dark matter candidates particularly attractive.

The DAMA signal can also be explained by the inelastic scattering of DM off nuclei mediated by a new massive $U(1)_x$ gauge boson. This exotic gauge boson can either be heavy and couple directly to the SM, or very light and hidden. In the heavy case, the new gauge boson must be somewhat leptophobic and have large couplings to quarks and the DM. Light gauge bosons can work if they have a GeV-range mass and couple to the SM through a small kinetic mixing with the photon. In contrast to the case of electroweak doublet DM, however, the correct nucleon scattering cross section and thermal relic density do not arise automatically, and must be arranged by hand.

Given that inelastic dark matter gives a compelling explanation for the DAMA result, it is of interest to understand what kind of models of IDM might work. The properties we need are clear. We need a particle of mass $\sim 100 - 1000\,\mathrm{GeV}$ whose real and imaginary (or Weyl) components are split by about $\sim 100\,\mathrm{keV}$. Such a small splitting violates a $U(1)_{DM}$ global symmetry that is preserved by a Dirac or complex scalar mass term. This makes such candidates technically natural.

We then address the question of overall naturalness. That is, why should the mass splitting be six orders of magnitude smaller than the overall mass scale? We found several candidate models. The first two work in the context of warped extra dimensions, where $U(1)_{DM}$ symmetry breaking can be sequestered. The symmetry breaking resides either in a large fermion Majorana mass or a small scalar holomorphic mass for a bulk singlet, that then mixes with an $SU(2)_L$ doublet dark matter candidate. The downside of these models is that we do not yet know if a warped extra dimension exists, or if the low UV scale needed in the scalar model is present.

The remaining models work in the context of supersymmetry. In the most compelling supersymmetric model, the smallness of the splitting arises through the mixing between an $SU(2)_L$ doublet fermion dark matter candidate and a singlet which directly couples to $U(1)_{DM}$ breaking. The smallness of the mixing is attributable in part to large $\tan\beta$. The

downside is that we do not know if weak-scale supersymmetry is present, or why there should be a minor conspiracy of small numbers to give the necessary suppression. Other supersymmetric models can work, but they generally require more assumptions or more complications to sufficiently isolate $U(1)_{DM}$ symmetry breaking.

We do not yet know if the DAMA signal will prove to be new physics. If it is, we conclude that inelastic dark matter particles are excellent candidates. Reasonable (but not completely obvious) assumptions then lead to acceptable models of inelastic dark matter. We are very fortunate in that upcoming results from XENON, CRESST, and other direct detection experiments should be able to help determine if such models are likely correct.

Acknowledgements

A   Appendix: Decoupling of KK Modes in the Warped Fermion Model

In this appendix we show that the effect of the bulk singlet KK modes can be neglected when calculating the DM mass splitting in the warped fermion model of section 4.1.1. Note that this is despite the fact that the zero mode and KK modes have a large mixing due to the Majorana mass terms (*i.e.*, $A_{00} \sim A_{mn}$). The key point is that the KK modes all have vector-like $U(1)_{DM}$ preserving masses, and are very inefficient at communicating $U(1)_{DM}$ breaking.

One can see this explicitly in the case of the first KK mode by including the couplings to the dark matter doublet as part of the mass matrix, and solving for the eigenvalues in the limit of a small Higgs VEV. For simplicity we can also neglect the Dirac mass of the doublet, which plays no role in the communication of $U(1)_{DM}$ breaking. The mass matrix is then

$$\mathscr{L} \supset -\frac{1}{2} \begin{pmatrix} \bar{S}_L^0 & \bar{S}_L^1 & \bar{S}_R^{1c} & \bar{D}_R^c \end{pmatrix} \begin{pmatrix} A_{00} & A_{01} & 0 & C_0 v \\ A_{01} & A_{11} & m_1 & C_1 v \\ 0 & m_1 & 0 & 0 \\ C_0 v & C_1 v & 0 & 0 \end{pmatrix} \begin{pmatrix} S_L^{0c} \\ S_L^{1c} \\ S_R^1 \\ D_R \end{pmatrix} + h.c., \qquad \text{(A.1)}$$

and the eigenvalues are determined from the roots of the characteristic polynomial $\text{Det}(M - \lambda I)$

$$\begin{aligned} 0 &= \lambda^4 - (A_{00} + A_{11})\lambda^3 - (C_0^2 v^2 + C_1^2 v^2 + m_1^2)\lambda^2 \\ &\quad + \left(A_{00}(m_1^2 + C_1^2 v^2) + A_{11} C_0^2 v^2 - 2 A_{01} C_0 C_1 v^2 \right) \lambda + m_1^2 C_0^2 v^2, \end{aligned} \qquad \text{(A.2)}$$

where we have used the fact that $A_{00}A_{11} - A_{01}^2 = 0$. In the limit that v^2 goes to 0, there is a zero eigenvalue corresponding to the doublet. Thus we expect that the eigenvalue is proportional to v^2. Plugging in $\lambda = xv^2$ and dropping terms of $O(v^4)$, we obtain

$$0 \approx xA_{00}m_1^2v^2 + m_1^2C_0^2v^2 + O(v^4) \tag{A.3}$$

so $x \approx \frac{-C_0^2}{A_{00}}$, and we see that at leading order the Majorana mass of the doublet is $\lambda \approx \frac{-C_0^2v^2}{A_{00}}$. This only depends on A_{00}, and is independent of A_{11} and A_{01} as we assumed in the estimates of section 4.1.1.

The leading corrections to this formula are proportional to $\sim \frac{C^4v^4}{Am^2}$ and are suppressed compared to the contribution from the zero mode by a factor $\sim \frac{v^2}{m^2}$. We have numerically checked that the effects of including more KK modes are also similarly suppressed, and that the sequence rapidly converges after the first few modes. We also note that this behavior is consistent with the results of Ref. [83].

B Appendix: Decoupling of Higher KK Modes in the Warped Scalar Model

In this appendix we will show that the effective coupling of singlet KK modes to the DM doublet C_n^{eff} becomes suppressed as $\sim 1/n$ for large n in the warped scalar model of section 4.1.2.

Substituting the form of the KK mode wavefunctions Eq. (4.21) into Eq. (4.35), we see that computing C_n^{eff} requires performing the integral

$$C_n^{eff} \simeq \sqrt{\frac{\pi m_n}{2}} \frac{\lambda e^{-\pi kR/2}}{\Delta} \int_{\pi R - \frac{\Delta}{2}}^{\pi R + \frac{\Delta}{2}} dy \left[J_\alpha(\frac{m_n}{k}e^{ky}) + b_\alpha(m_n)Y_\alpha(\frac{m_n}{k}e^{ky}) \right]. \tag{B.1}$$

Close to $y = \pi R$, the integrand is completely dominated by J_α. For large argument (large n), this Bessel function can be approximated as

$$J_\alpha(\frac{m_n}{k}e^{ky}) \approx \sqrt{\frac{2k}{\pi m_n e^{ky}}} \cos\left(\frac{m_n}{k}e^{ky} - \frac{\pi}{2}(\alpha + \frac{1}{2}) \right). \tag{B.2}$$

Changing variables to $z = \frac{1}{k}e^{ky}$ then gives

$$C_n^{eff} \simeq \frac{\lambda e^{-\pi kR/2}}{k\Delta} \int_{z_-}^{z_+} dz\, z^{-\frac{3}{2}} \cos\left(m_n z - \frac{\pi}{2}(\alpha + \frac{1}{2}) \right), \tag{B.3}$$

where $z_\pm = \frac{1}{k}e^{k(\pi R \pm \frac{\Delta}{2})}$. The cosine rapidly oscillates over the brane thickness at large n, while the $z^{-\frac{3}{2}}$ piece is relatively stable. Approximating the stable piece by its central value and performing the integral, one obtains

$$C_n^{eff} \approx \frac{\lambda \sqrt{k}e^{-2\pi kR}}{m_n\Delta} \left[\sin\left(m_n z_+ - \frac{\pi}{2}(\alpha + \frac{1}{2}) \right) - \sin\left(m_n z_- - \frac{\pi}{2}(\alpha + \frac{1}{2}) \right) \right], \tag{B.4}$$

39

and then one can place an approximate upper bound the magnitude of C_n^{eff},

$$|C_n^{eff}| \lesssim \frac{\lambda\sqrt{k}e^{-2\pi kR}}{m_n\Delta}. \tag{B.5}$$

Thus, we see that the magnitude of C_n^{eff} falls roughly as $\sim 1/n$ as we set out to show.

References

[1] R. Bernabei *et al.* [DAMA Collaboration], Eur. Phys. J. C **56**, 333 (2008) [arXiv:0804.2741 [astro-ph]].

[2] M. W. Goodman and E. Witten, Phys. Rev. D **31**, 3059 (1985).

[3] A. K. Drukier, K. Freese and D. N. Spergel, Phys. Rev. D **33**, 3495 (1986).

[4] Z. Ahmed *et al.* [CDMS Collaboration], [arXiv:0802.3530 [astro-ph]].

[5] J. Angle *et al.* [XENON Collaboration], Phys. Rev. Lett. **100**, 021303 (2008) [arXiv:0706.0039 [astro-ph]].

[6] G. Gelmini and P. Gondolo, [arXiv:hep-ph/0405278]; P. Gondolo and G. Gelmini, Phys. Rev. D **71**, 123520 (2005) [arXiv:hep-ph/0504010].

[7] F. Petriello and K. M. Zurek, JHEP **0809**, 047 (2008) [arXiv:0806.3989 [hep-ph]].

[8] S. Chang, A. Pierce and N. Weiner, [arXiv:0808.0196 [hep-ph]].

[9] M. Fairbairn and T. Schwetz, [0808.0704 [hep-ph]].

[10] C. Savage, G. Gelmini, P. Gondolo and K. Freese, [0808.3607 [astro-ph]].

[11] D. Tucker-Smith and N. Weiner, Phys. Rev. D **64**, 043502 (2001) [arXiv:hep-ph/0101138].

[12] D. Tucker-Smith and N. Weiner, Nucl. Phys. Proc. Suppl. **124**, 197 (2003) [arXiv:astro-ph/0208403].

[13] D. Tucker-Smith and N. Weiner, Phys. Rev. D **72**, 063509 (2005) [arXiv:hep-ph/0402065].

[14] S. Chang, G. D. Kribs, D. Tucker-Smith and N. Weiner, [arXiv:0807.2250 [hep-ph]].

[15] N. Arkani-Hamed, D. P. Finkbeiner, T. Slatyer and N. Weiner, [arXiv:0810.0713 [hep-ph]];

[16] S. Chang, G. D. Kribs, D. Tucker-Smith and N. Weiner, in progress.

[17] E. Kuflik, in progress.

[18] O. Adriani *et al.*, [arXiv:0810.4995 [astro-ph]].

[19] J. Chang *et al.*, Nature **456**, 362 (2008).

[20] S. Torii *et al.*, [arXiv:0809.0760 [astro-ph]].

[21] G. Weidenspointner *et al.*, [arXiv:astro-ph/0601673].

[22] D. P. Finkbeiner, Astrophys. J. **614**, 186 (2004) [arXiv:astro-ph/0311547].

[23] G. Dobler and D. P. Finkbeiner, Astrophys. J. **680**, 1222 (2008) [arXiv:0712.1038 [astro-ph]].

[24] D. Hooper, D. P. Finkbeiner and G. Dobler, Phys. Rev. D **76**, 083012 (2007) [arXiv:0705.3655 [astro-ph]].

[25] E. Ponton and L. Randall, arXiv:0811.1029 [hep-ph].

[26] N. Arkani-Hamed, A. Delgado and G. F. Giudice, Nucl. Phys. B **741**, 108 (2006) [arXiv:hep-ph/0601041].

[27] G. Jungman, M. Kamionkowski and K. Griest, Phys. Rept. **267**, 195 (1996) [arXiv:hep-ph/9506380].

[28] G. Bertone, D. Hooper and J. Silk, Phys. Rept. **405**, 279 (2005) [arXiv:hep-ph/0404175].

[29] R. H. Helm, Phys. Rev. **104**, 1466 (1956).

[30] J. D. Lewin and P. F. Smith, Astropart. Phys. **6**, 87 (1996).

[31] G. Duda, A. Kemper and P. Gondolo, JCAP **0704**, 012 (2007) [arXiv:hep-ph/0608035].

[32] M. C. Smith *et al.*, Mon. Not. Roy. Astron. Soc. **379**, 755 (2007) [arXiv:astro-ph/0611671].

[33] W. Dehnen and J. Binney, Mon. Not. Roy. Astron. Soc. **298**, 387 (1998) [arXiv:astro-ph/9710077].

[34] J. Binney and S.Tremaine, "Galactic Dynamics," Princeton University Press, Second Ed., 2008.

[35] G. Gelmini and P. Gondolo, Phys. Rev. D **64**, 023504 (2001) [arXiv:hep-ph/0012315].

[36] R. Bernabei *et al.*, Eur. Phys. J. C **53**, 205 (2008) [arXiv:0710.0288 [astro-ph]].

[37] D. S. Akerib *et al.* [CDMS Collaboration], Phys. Rev. Lett. **93**, 211301 (2004) [arXiv:astro-ph/0405033].

[38] D. S. Akerib *et al.* [CDMS Collaboration], Phys. Rev. Lett. **96**, 011302 (2006) [arXiv:astro-ph/0509259].

[39] G. Angloher *et al.*, [arXiv:0809.1829 [astro-ph]].

[40] V. N. Lebedenko *et al.*, [arXiv:0812.1150 [astro-ph]].

[41] H. S. Lee. *et al.* [KIMS Collaboration], Phys. Rev. Lett. **99**, 091301 (2007) [arXiv:0704.0423 [astro-ph]].

[42] G. J. Alner *et al.*, Astropart. Phys. **28**, 287 (2007) [arXiv:astro-ph/0701858].

[43] G. Angloher *et al.*, Astropart. Phys. **23**, 325 (2005) [arXiv:astro-ph/0408006].

[44] J. March-Russell, C. McCabe and M. McCullough, [arXiv:0812.1931 [astro-ph]].

[45] A. M. Green, Phys. Rev. D **68**, 023004 (2003) [Erratum-ibid. D **69**, 109902 (2004)] [arXiv:astro-ph/0304446].

[46] S. H. Hansen, B. Moore, M. Zemp and J. Stadel, JCAP **0601**, 014 (2006) [arXiv:astro-ph/0505420].

[47] M. Vogelsberger *et al.*, [arXiv:0812.0362 [astro-ph]].

[48] M. Cirelli, N. Fornengo and A. Strumia, Nucl. Phys. B **753**, 178 (2006) [arXiv:hep-ph/0512090].

[49] C. Savage, P. Gondolo and K. Freese, Phys. Rev. D **70**, 123513 (2004) [arXiv:astro-ph/0408346].

[50] R. Bernabei *et al.*, Phys. Rev. D **77**, 023506 (2008) [arXiv:0712.0562 [astro-ph]].

[51] Y. Bai and Z. Han, [arXiv:0811.0387 [hep-ph]].

[52] P. J. Fox and E. Poppitz, [arXiv:0811.0399 [hep-ph]].

[53] M. Cirelli, M. Kadastik, M. Raidal and A. Strumia, [arXiv:0809.2409 [hep-ph]].

[54] I. Cholis, G. Dobler, D. P. Finkbeiner, L. Goodenough and N. Weiner, [arXiv:0811.3641 [astro-ph]].

[55] G. Belanger, F. Boudjema, A. Pukhov and A. Semenov, Comput. Phys. Commun. **176**, 367 (2007) [arXiv:hep-ph/0607059]; arXiv:0803.2360 [hep-ph].

[56] T. Hur, H. S. Lee and S. Nasri, Phys. Rev. D **77**, 015008 (2008) [arXiv:0710.2653 [hep-ph]].

[57] J. L. Feng and J. Kumar, [arXiv:0803.4196 [hep-ph]].

[58] M. Fairbairn and J. Zupan, [arXiv:0810.4147 [hep-ph]].

[59] K. M. Zurek, [arXiv:0811.4429 [hep-ph]].

[60] L. J. Hall, T. Moroi and H. Murayama, Phys. Lett. B **424**, 305 (1998) [arXiv:hep-ph/9712515].

[61] O. Stelzer-Chilton [CDF and D0 Collaboration], [arXiv:0810.4754 [hep-ex]].

[62] C. Schwanenberger [CDF and D0 Collaboration], PoS **HEP2005**, 349 (2006) [arXiv:hep-ex/0602048].

[63] [LEP Collaboration and ALEPH Collaboration and DELPHI Collaboration and], [arXiv:hep-ex/0312023].

[64] B. Holdom, Phys. Lett. B **259**, 329 (1991).

[65] Y. Umeda, G. C. Cho and K. Hagiwara, Phys. Rev. D **58**, 115008 (1998) [arXiv:hep-ph/9805447]; G. C. Cho, K. Hagiwara and Y. Umeda, Nucl. Phys. B **531**, 65 (1998) [Erratum-ibid. B **555**, 651 (1999)] [arXiv:hep-ph/9805448].

[66] T. Appelquist, B. A. Dobrescu and A. R. Hopper, Phys. Rev. D **68**, 035012 (2003) [arXiv:hep-ph/0212073].

[67] M. S. Carena, A. Daleo, B. A. Dobrescu and T. M. P. Tait, Phys. Rev. D **70**, 093009 (2004) [arXiv:hep-ph/0408098].

[68] J. Kumar and J. D. Wells, Phys. Rev. D **74**, 115017 (2006) [arXiv:hep-ph/0606183].

[69] P. Langacker, [arXiv:0801.1345 [hep-ph]].

[70] T. G. Rizzo, [arXiv:hep-ph/0610104].

[71] B. Holdom, Phys. Lett. B **166**, 196 (1986).

[72] K. R. Dienes, C. F. Kolda and J. March-Russell, Nucl. Phys. B **492**, 104 (1997) [arXiv:hep-ph/9610479]; K. S. Babu, C. F. Kolda and J. March-Russell, Phys. Rev. D **57**, 6788 (1998) [arXiv:hep-ph/9710441].

[73] C. Boehm and P. Fayet, Nucl. Phys. B **683**, 219 (2004) [arXiv:hep-ph/0305261]; C. Boehm, P. Fayet and J. Silk, Phys. Rev. D **69**, 101302 (2004) [arXiv:hep-ph/0311143]; P. Fayet, Phys. Rev. D **70**, 023514 (2004) [arXiv:hep-ph/0403226]; C. Bouchiat and P. Fayet, Phys. Lett. B **608**, 87 (2005) [arXiv:hep-ph/0410260];

[74] D. Feldman, Z. Liu and P. Nath, Phys. Rev. Lett. **97**, 021801 (2006) [arXiv:hep-ph/0603039].

[75] W. F. S. Chang, J. N. Ng and J. M. S. Wu, Phys. Rev. D **74**, 095005 (2006) [arXiv:hep-ph/0608068].

[76] M. Pospelov, [arXiv:0811.1030 [hep-ph]].

[77] M. Pospelov, A. Ritz and M. B. Voloshin, Phys. Lett. B **662**, 53 (2008) [arXiv:0711.4866 [hep-ph]].

[78] P. Gondolo and G. Gelmini, Nucl. Phys. B **360**, 145 (1991).

[79] J. Edsjo and P. Gondolo, Phys. Rev. D **56**, 1879 (1997) [arXiv:hep-ph/9704361].

[80] C. Arina, F. Bazzocchi, N. Fornengo, J. C. Romao and J. W. F. Valle, Phys. Rev. Lett. **101**, 161802 (2008) [arXiv:0806.3225 [hep-ph]].

[81] P. Kumar, arXiv:0809.2610 [hep-ph].

[82] L. Randall and R. Sundrum, Phys. Rev. Lett. **83**, 3370 (1999) [arXiv:hep-ph/9905221]; L. Randall and R. Sundrum, Phys. Rev. Lett. **83**, 4690 (1999) [arXiv:hep-th/9906064].

[83] S. J. Huber and Q. Shafi, Phys. Lett. B **583**, 293 (2004) [arXiv:hep-ph/0309252].

[84] G. Perez and L. Randall, arXiv:0805.4652 [hep-ph].

[85] T. Gherghetta and A. Pomarol, Nucl. Phys. B **586**, 141 (2000) [arXiv:hep-ph/0003129].

[86] I. I. Kogan, S. Mouslopoulos, A. Papazoglou and G. G. Ross, Nucl. Phys. B **595**, 225 (2001) [arXiv:hep-th/0006030].

[87] G. Moreau, Eur. Phys. J. C **40**, 539 (2005) [arXiv:hep-ph/0407177].

[88] K. L. McDonald, Phys. Rev. D **77**, 124046 (2008) [arXiv:0804.0654 [hep-th]].

[89] H. Davoudiasl, G. Perez and A. Soni, Phys. Lett. B **665**, 67 (2008) [arXiv:0802.0203 [hep-ph]].

[90] H. Davoudiasl, [arXiv:0810.0194 [hep-ph]].

[91] J. L. Hewett, F. J. Petriello and T. G. Rizzo, JHEP **0209**, 030 (2002) [arXiv:hep-ph/0203091].

[92] A. Pomarol, Phys. Lett. B **486**, 153 (2000) [arXiv:hep-ph/9911294].

[93] G. R. Dvali, G. Gabadadze and M. A. Shifman, Phys. Lett. B **497**, 271 (2001) [arXiv:hep-th/0010071].

[94] H. Georgi, A. K. Grant and G. Hailu, Phys. Lett. B **506**, 207 (2001) [arXiv:hep-ph/0012379].

[95] M. S. Carena, T. M. P. Tait and C. E. M. Wagner, Acta Phys. Polon. B **33**, 2355 (2002) [arXiv:hep-ph/0207056].

[96] J. Erler, Nucl. Phys. B **586**, 73 (2000) [arXiv:hep-ph/0006051].

[97] D. E. Morrissey and J. D. Wells, Phys. Rev. D **74**, 015008 (2006) [arXiv:hep-ph/0512019].

[98] D. Suematsu, JHEP **0611**, 029 (2006) [arXiv:hep-ph/0606125].

[99] D. Hooper and K. M. Zurek, Phys. Rev. D **77**, 087302 (2008) [arXiv:0801.3686 [hep-ph]].

[100] E. J. Chun and J. C. Park, [arXiv:0812.0308 [hep-ph]].

[101] N. Arkani-Hamed and N. Weiner, [arXiv:0810.0714 [hep-ph]].

[102] G. F. Giudice and A. Masiero, Phys. Lett. B **206**, 480 (1988).